Technische Universität Dresden
Fakultät für Maschinenwesen
Institut für Energietechnik
Professur für Termische Energiemaschinen und -anlagen
Prof. Dr.-Ing. Uwe Gampe

D 420/18

DIPLOMA THESIS

Topic:	**"Conceptual design of an integrated waste heat recovery plant for municipal and industrial applications"**
Name:	Patricia Álvarez Salamanqués
Mentors:	Dr.-Ing. Mario Raddatz Dr.-Ing. Guntram Buchheim
Supervising university teacher:	Prof. Dr.-Ing. Uwe Gampe

TECHNISCHE UNIVERSITÄT DRESDEN

Fakultät für Maschinenwesen

Subject of Master Thesis **D 420/18**

Name **Mrs. Patricia Álvarez Salamanqués**

Home University / Course **Universidad de Valladolid / Industrial Engineering**

Task: **"Conceptual design of an integrated waste heat recovery plant for municipal and industrial applications"**

The increased usage of industrial and urban waste heat is an essential contribution to the global warming and conversion of primary energy resources. Unfortunately, the temperature level of such energy sources is moderate, so that the achievable efficiencies of the thermodynamic processes are limited. Lower temperature heat sources can favourably be utilized by Organic Rankine Cycles (ORC).

In this work, the state of heat recovery in Central and Southern Europe shall be compared to the supply of waste heat. ORC's for the heat sources with the greatest economic potential shall be analysed for their applicability. This can be done by conducting examples.

Based on these requirements, it is necessary to design a compact integrated system, which includes the machines and the generators. It is essential to determine the main dimensions of the compact integrated system.

Specifically, the following tasks have to be performed:

- Market analysis on the usage of waste heat in industrial and urban sector
- Characterisation of available heat sources
- Analysis of existing comparable facilities in terms of cost effectiveness and complexity
- Selection and calculating process, determines the most important process parameters and fluids
- Determining the main dimensions of the integrated turbomachinery and the generator

The results should be summarized as a technical report either in English or German, the calculation documents are to be enclosed. The scope of work can be limited or extended depending on the results achieved and in mutual agreement with the supervisor.

Mentors Dr.-Ing. Mario Raddatz / Dr.-Ing. Guntram Buchheim

Handed out: 2018-04-30 Deadline: 2018-09-28

Prof. Dr.-Ing. Uwe Gampe
Supervising university teacher

Abstract

Increasing attention is being paid in the use of low-grade waste heat sources, which are broad but often undeveloped. This is not only for its potential in reducing fossil fuel consumption and alleviating environmental concerns, but also because of its potential to optimize companies' resources. Organic Rankine Cycle (ORC) is the most widespread technology to take advantage of lower temperature heat sources.

The aim of the present work is finding a suitable solution for a compact integrated ORC turbomachine based on the necessities of the existing industry. Therefore, a market analysis in the use of waste heat in Europe was carried out. After deducing the middle of the market, which was established as the heat source to recover, several simulations were executed in order to determine the optimal cycle conditions. Finally, to ensure the feasibility of the whole system, the definition of the components main dimensions is as well essential. Thus, a preliminary design was performed based on Cordier diagram.

Key words

Organic Rankine Cycle (ORC), waste heat, low-grade heat, turbomachinery

Index

Figures index

Tables index

Equations index

Symbol and abbreviation directories

Symbol directory

Symbol	**Meaning**	**Units**
$\dot{m}$	Mass flow	kg/s
P	Pressure	bar
T	Temperature	°C
s	Entropy	kJ/kg K
h	Specific enthalpy	kJ/kg
h_s	Isentropic specific enthalpy	kJ/kg
X	Steam rate	
v	Specific volume	m^3/kg
ρ	Density	kg/m^3
$\dot{Q}_{evaporator}$	Heat transferred in the evaporator	kW
$\dot{Q}_{condenser}$	Heat transferred in the condenser	kW
$\dot{W}_{turbine}$	Work generated by the turbine	kW
$\dot{W}_{pump}$	Work required in the pump	kW
$\eta_{turbine}$	Turbine isentropic efficiency	
η_{pump}	Pump isentropic efficiency	
η_{thm}	Thermal efficiency	
ETA	Efficiency considering the losses in the mechanical to electrical conversion	
ξ	Measure of the “dryness” or “wetness” of a working fluid	
K	Global heat transfer coefficient	W/m^2 K
A	Heat transmission area	m^2
$\dot{V}$	Volumetric flowrate	m^3/s
Y	Specific head	Pa m^3/kg
$D \mid d$	Impeller diameter	mm
$N \mid n$	Rotation speed	1/min
u	Circumferential speed	m/s

C_m	Meridian velocity	m/s
$B \mid b$	Width of the impeller blade	mm
φ	Flow number	
ψ	Head number	

Abbreviation directory

ORC	Organic Rankine Cycle
MTOE	Million Tonnes of Oil Equivalent
$GtCO_2$	Giga Tonnes of CO_2
HC	Hydrocarbon
PCF	Perfluorocarbon
CFC	Chlorofluorocarbon
HFC	Hydrofluorocarbon
HCFC	Hydrochlorofluorocarbon
HFO	Hydrofluoroolefin
OEL	Occupational Exposure Limit
TLV	Threshold Limit Value
LFL	Lower Flammability Limit
TWA	Time Weighted Average
ALT	Atmospheric Lifetime
ODP	Ozone Depletion Potential
GWP	Global Warming Potential

1. Introduction

Steam Rankine cycles driven by fossil fuels are still nowadays the dominant power supply method. However, as it is known to all, the accelerated consumption of fossil fuels has caused many serious environmental problems such as air pollution, global warming, ozone layer depletion and acid rain. Finding an effective procedure to utilize low and medium temperature heat sources, which are vast but undeveloped, is one of the most promising solutions to alleviate the energy shortage and environmental pollution struggles. In addition to this, other kind of problems are encountered when using water as working fluid for steam Rankine cycle:

- Necessity of superheating to prevent condensation during the expansion
- Risk of erosion of the turbine blades
- Excessive pressure in the evaporator
- Complex and expensive turbines

Various thermodynamic cycles such as the organic Rankine cycle (ORC), supercritical Rankine cycle, Kalina cycle and trilateral flash cycle have been proposed and examined for the conversion of low-grade heat sources into electricity. Compared with the Kalina cycle's complex system structure, trilateral flash cycle's difficult two-phase expansion and supercritical Rankine cycle's high operating pressure, organic Rankine cycle seems to be an appealing alternative to take advantage of the low-temperature heat sources available in the industry.

This cycle has the same system configuration as the steam Rankine cycle but, instead of water as the working fluid, it is composed with organic substances characterized by having low boiling temperatures. This system is able to exploit several types of heat sources, including industrial waste heat, solar, geothermal, biomass and ocean energies, etc. Meanwhile, in order to improve energy utilization, it can be easily combined with other thermodynamic cycles, such as the thermoelectric generator, fuel cell, internal combustion engine, micro turbine, seawater desalination system, etc [1].

In recent years, the use these low-grade heat sources such as geothermal resources, exhaust gases of gas turbines and waste heat from industrial areas, has received increasing attentions. This is not only for its potential in reducing fossil fuel consumption and alleviating environmental concerns, but also to optimize companies' resources and profit in producing electricity from the heat currently wasted due to their regular processes. In essence, the principal advantage of an organic Rankine cycle (ORC) system, using an organic fluid instead of water, is its potential feasibility for low-grade heat recovery systems. These classic Rankine cycles are not efficient enough for temperatures below 400 ^{o}C.

Since conventional steam power cycles cannot give a better performance to recover low-grade waste heat, the organic Rankine cycle (ORC) is proposed to recover these low temperature sources into electricity, mainly in the temperature range from 100 to 400 ^{o}C. Although the most important advantages of this cycle have been already mentioned, there are several assets,

among which highlight: economical utilization of energy resources, lower equipment requirements and emissions reduction of CO, CO_2, NO_X as well as other atmospheric pollutants.

1.1. Background in the utilization of low-grade waste heat

The ORC is not a new concept, much research has been conducted on it, especially from 2000 onwards due to the raised attention to low-medium temperature heat recovery. This rise in the amount of studies is caused primarily by the growing concerns about the environmental impact and by the need for efficiency improvement of the energy systems. Imran et al. [2] describe, using the Scopus Elsevier database and the Science Citation Index Expanded, the contribution of researchers around the world in the field of organic Rankine cycle during the period 2000-2016. Based on this paper, some of the most outstanding and recent researches have been collected categorized by topic in *Table 1*.

Topic	Main authors and papers
Use of ORC power systems for waste heat recovery from internal combustion engines	Lion et al. [3] Sprouse et al. [4] Saidur et al. [5]
Small-scale applications of ORC power systems	Tocci et al. [6] Rahbar et al. [7]
Review and selection criteria of pure working fluids	Bao and Zhao [1] Chen et al. [8]
Potential and challenges of the use of zeotropic mixtures for ORC applications	Modi and Haglind [9] Abadi and Kim [10]
Thermal stability of the working fluids	Dai et al. [11]
Selection and performance of expanders for ORC power systems	Imran et al. [12] Song et al. [13] Bao et al. [1]
Generalized overview of cycle configurations and cycle architectures	Lecompte et al. [14]
Potential heat sources and categorization for ORC applications	Zhai et al. [15]

Table 1. Summary with the main papers, gathered by topic; based on [2].

One of the main issues that should be considered is the selection of a proper working fluid from the many different working fluids for recovering a given waste heat. Regarding this topic, apart from the comprehensive reviews about pure working fluids developed by Bao et al. [1] and Chen et al. [8], several additional studies have been carried out regarding this topic.

Among them, Drescher and Bruggemann [16] investigated the ORC in solid biomass power and heat plants. They suggested a method to determine suitable thermodynamic fluids for ORCs in biomass plants and found that the family of alkybenzenes performed the highest efficiency.

Other example is that of Chen et al. [17], who examined the performance of CO_2 trans-critical power cycle using energy from low-grade waste heat in comparison to an ORC using R123 as

working fluid. They detected that when using the low-grade heat source with equal mean thermodynamic heat rejection temperature, the carbon dioxide trans-critical power cycle had a slightly higher power output than the ORC. Liu et al. [18] described, as well, the performance of organic Rankine cycles subjected to the influence of working fluids. They examined the effects of various working fluids on the thermal efficiency and on the total heat recovery efficiency.

In addition, Hung et al. [19] analyzed working fluids for organic Rankine cycles to recover waste heat, including: benzene, toluene, p-xylene, R113 and R123. They realized that p-xylene displayed the highest efficiency while benzene resulted in the lowest, and p-xylene had the lowest irreversibility in recovering a high temperature waste heat while R113 and R123 had a better performance in recovering a low temperature waste heat.

The results showed that for operation between isobaric curves, the system efficiency increased for wet fluids and decreased for dry fluids while the isentropic fluid achieved an approximately constant value for high turbine inlet temperatures, and isentropic fluids were most suitable for recovering low temperature waste heat. However, there is an important threshold of this study: it is not easy to evaluate the performance of the ORC with different working fluids under different operating parameters. It could turn out into better or worse performance of ORCs with different working fluids under their optimization conditions.

As it is described by Imran et al. [2], there are many the publications and patents that have been developed in the last years regarding organic Rankine cycles (see *Figure 1*). The published articles were originated in more than 71 countries. In the graph, the rapid increase in papers and publications in the year 2008 and thereafter should be emphasized. This could be connected to the growing concerns about the environmental impact as well as to the need for efficiency improvements in the energy systems.

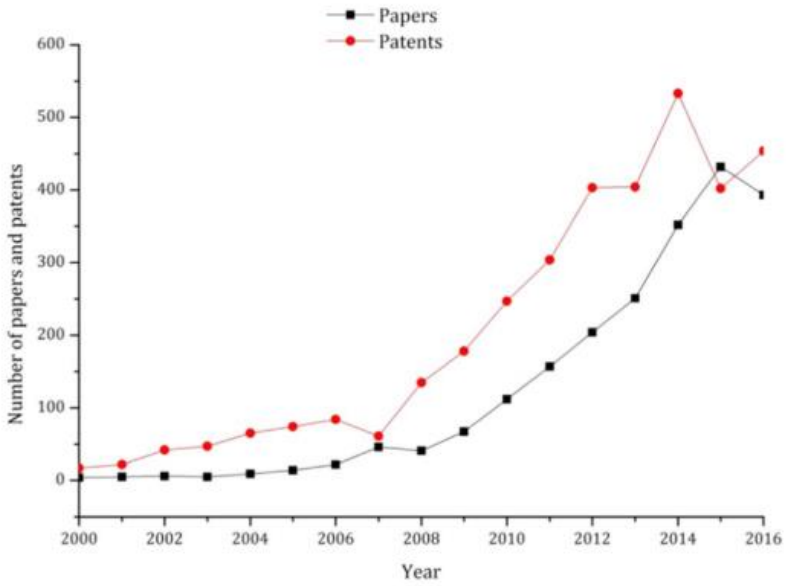

Figure 1. Timeline of papers and patents about ORC systems between 2000 and 2016 [2].

As these issues started to be considered by several governments and official institutions, many funds were intended to promote the rise of researches and enhancements in this field. Within

the European Union, the industrial sector holds nearly a quart of the whole energy consumption and the fifth part of the greenhouse gas emissions. “LOVE” (Low-temperature heat valorization towards electricity production) is a project supported with European funds to find different ways to take advantage, with efficiency, of this residual heat. This study consisted on finding heat sources at low temperature (less than 120 ^{o}C) and developing profitable technologies with the purpose of turning this heat into electricity. The members of the consortium based their work in pinch analysis and in the process integration. They incorporated two ORC systems of 100 kWe in two pilot cement plants [20].

Furthermore, there has been done likewise much research with the purpose of finding innovative technologies, different from ORC turbomachinery, which could make great utilization of this waste heat. For instance, a research group from Pennsylvania State University (United States) developed a battery based in ammonia. This consists in copper electrodes with added ammonia only to the anolyte, the electrolyte that surrounds the anode. Fang Zhang, a post-doctoral researcher in environmental engineering at the university, explained the procedure: "The battery works until the reaction spends the ammonia necessary to form complexes in the electrolyte near the anode or depletes the copper ions in the electrolyte near the cathode. Then the reaction stops”. Using low-grade residual heat from an external source, researchers distil ammonia from the effluent remaining in the battery's anolyte and then return it to the original battery cathode chamber. The flow of liquid ammonia can convert thermal energy into electrical energy in the battery [21].

As it has been previously explained, it is common that current heat recovery systems use Organic Rankine Cycle (ORC) technology to generate electricity using waste heat from manufacturing plants. Although this technology works properly at temperatures ranging between 200 and 300 °C, its capacity to generate electricity from hot water at less than 100 °C is quite limited. For that reason, other research project financed with European funds is “The Exergyn Drive” [22] which has developed a technology that transforms low-grade waste heat at lower temperatures than 100 ^{o}C in an efficient way.

The factor that enables the entire process of generating electrical or mechanical energy from residual heat at low temperature, is the use of a shape memory alloy called “nitinol”. This material goes through a transition phase when it is heated to temperatures below 100 ^{o}C and returns to its original shape when cooled. “Depending on the conditions, this system can offer a better performance than the ORC by a factor of three to six at temperatures below 100 °C, which makes its commercialization viable. In addition, this technology is not based on the use of heat exchangers, which means that the engine can be more compact and does not require the use of toxic gasses” says Dr. O'Toole [22].

1.2. Main objectives

In the section above some of the research and attempts developed to optimize the utilization of low-grade waste heat sources, currently misused and released to the atmosphere, have been mentioned, emphasizing the significance of this task. The purpose of the present work, therefore, is finding a suitable solution for an ORC turbomachine based on the necessities of the

existing industry, describing not only its main thermodynamic parameters, but also the preliminary criteria for the equipment required, including the engines (turbine and pump).

The first objective is carrying out a research on the waste heat data available in Europe, towards a market analysis of the low-grade heat sources offered by the industry. The main parameters to be examined through this market analysis should be the common range of temperature depending on the industry sector, temperature level, heat carrier, power that could be supplied for the ORC turbomachine and the total energy per year and range of temperature. Departing from this data it is possible to analyse the most frequent conditions of the waste heat in the industry, leading to the middle of the market definition.

After the waste heat market analysis is concluded, the following objective consists in identifying the optimum cycle for the ORC system operation. In order to study that, several simulations in Ebsilon software will be undertaken. The middle of the market deduced from the market analysis is the input condition established at the evaporator device in the model (temperature level, heat power and heat carrier).

As a conclusion for the simulations in Ebsilon, a working fluid and the cycle parameters need to be selected, taking into account the best performance accomplished. Subsequently, the final objective is analysing the main dimensions of the system components, so that it is possible to verify the whole system feasibility. Thus, an estimation of the heat exchangers sizes as well as a preliminary design of both engines (turbine and pump) needs to be assessed.

1.3. Description of the thermodynamic cycle

The ORC system is composed of the following elements: evaporator, turbine, condenser and pump, as shown in *Figure 2*.

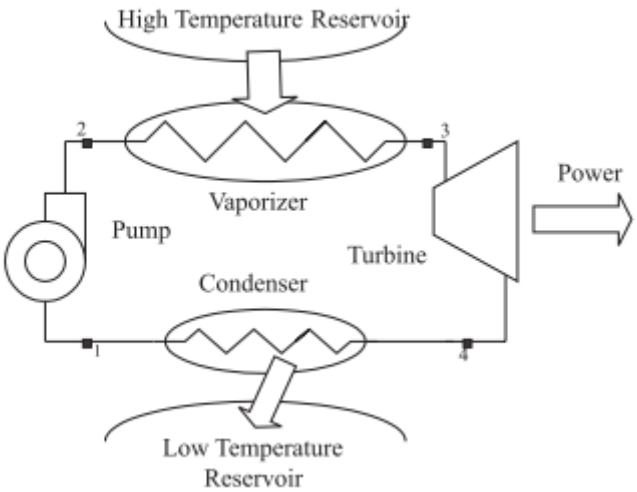

Figure 2. Main elements of the ORC cycle [19].

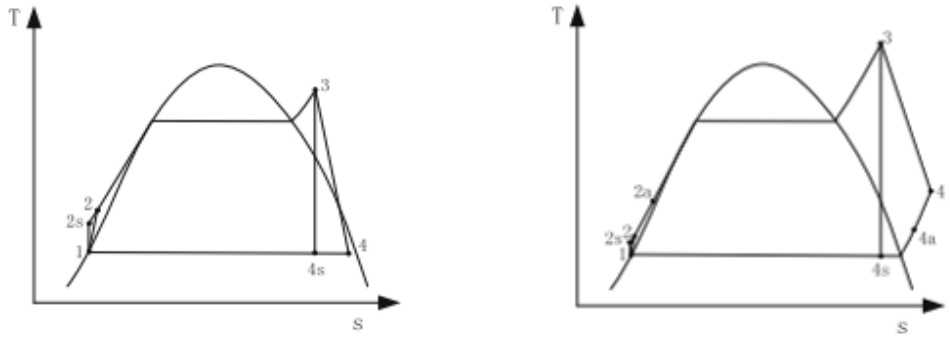

Figure 3. a) A type of ORC with negative slope of saturated vapor curve and wet vapor at the turbine outlet. b) A type of ORC with negative slope of saturated vapor curve and superheated vapor at the turbine inlet [23].

It can be classified in two groups according to the level of turbine inlet pressure, including supercritical ORCs and subcritical ORCs. The subcritical ORCs are also divided in three different groups according to the shape of saturated vapor curve in the temperature versus entropy diagram: negative slope, positive slope or vertical. In *Figure 3* two types of ORC processes with the negative slope of the saturated vapor curve in the T-S diagram are shown.

As it is presented in *Figure 3.a*, the working fluid leaves the condenser as saturated liquid (state point 1). Then, it is compressed by the pump to the sub-critical pressure (state point 2) desired in the heat addition process. The working fluid is heated in the evaporator until it becomes superheated vapor (state point 3). The superheated vapor flows into the turbine and is expanded to the condensing pressure (state point 4). At the condensing pressure, the working fluid lies in the two-phase region. The two-phase fluid passes through the condenser where heat is removed until it becomes a saturated liquid (state point 1). The processes in *Figure 3.b* are similar to those in *Figure 3.a,* with the only difference that the state point 4 after expansion in the turbine lies in the superheated vapor region.

Figure 4 shows the other two types of ORC processes: with the positive slope of the saturated vapor curve in the T-S diagram. The state points 1 and 2 correspond to the ORC system in *Figure 3.* Starting from state 2, the working fluid is heated in the evaporator at constant sub-critical pressure until it becomes saturated (state point 3) in *Figure 4.a* or it is superheated (state point 3) in *Figure 4.b.* Then, it is expanded to state point 4, which is always in the superheated vapor region.

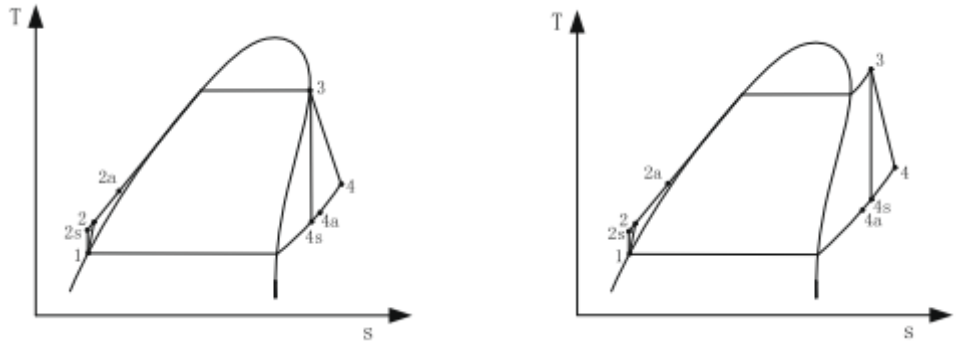

Figure 4. a) ORC with non-negative slope of saturated vapor curve and saturated vapor at the turbine inlet. b) ORC with non-negative slope of saturated vapor curve and superheated vapor at the turbine inlet [23].

In the above cycles, if the temperature T_4 is markedly higher than the temperature T_1, it may be rewarding to implement an internal heat exchanger into the cycles as shown in *Figure 5*. This heat exchanger is also represented in *Figure 3* and *Figure 4* by the additional state points 4a and 2a. The turbine exhaust flows into the internal heat exchanger and cools in the heat exchanger through the process (4-4a) by transferring heat to the compressed liquid that is heated in the process (2-2a) [23].

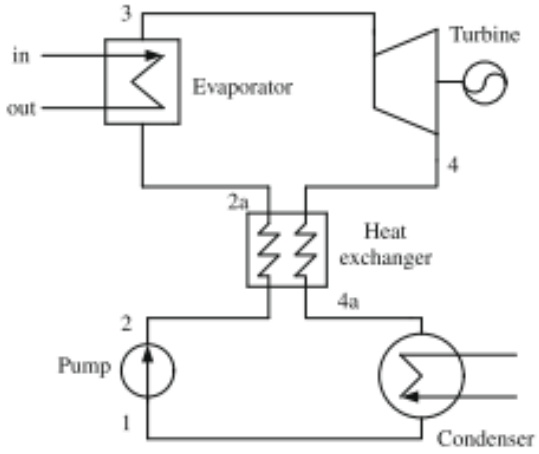

Figure 5. The ORC system with internal heat exchanger [23].

Each process in the ORC can be described as follows:

- *EVAPORATOR*, process 2 to 3: this is the constant pressure heat absorption in the evaporator. The heat transferred from the waste heat to the working fluid can be described as:

$$\dot{Q}_{evaporator} = \dot{m} \cdot (h_3 - h_2)$$

Equation 1. Heat transferred in the evaporator.

If the internal heat exchanger is added, the process is 2a to 3 and the amount of heat transferred is presented by:

$$\dot{Q}_{evaporator} = \dot{m} \cdot (h_3 - h_{2a})$$

- *TURBINE*, process 3 to 4: although ideally this could be an isentropic process 3-4s, it is about a non-isentropic expansion process. This is due to the efficiency of the energy transformation in the turbine never reaches 100%, and the state of the working fluid at the turbine outlet is indicated by state point 4, instead of 4s. The isentropic efficiency of the turbine can be expressed as:

$$\eta_{turbine} = \frac{h_3 - h_4}{h_3 - h_{4s}}$$

Equation 2. Isentropic efficiency in the turbine.

The power generated by the turbine can be given as:

$$\dot{W}_{turbine} = \dot{m} \cdot (h_3 - h_4)$$

Equation 3. Work power in the turbine.

- *CONDENSER*, process 4 to 1: this is constant pressure heat rejection process in the condenser whose heat flow is described by:

$$\dot{Q}_{condenser} = \dot{m} \cdot (h_4 - h_1)$$

Equation 4. Heat transferred in the condenser.

If the internal heat exchanger is added, the process is 2a to 3 and the amount of heat transferred is presented by:

$$\dot{Q}_{condenser} = \dot{m} \cdot (h_{4a} - h_1)$$

- *PUMP*, process 1 to 2: similar to the turbine, this is a non-isentropic compression process in the liquid pump. The isentropic efficiency of the pump can be expressed as:

$$\eta_{pump} = \frac{h_{2s} - h_1}{h_2 - h_1}$$

Equation 5. Isentropic efficiency in the pump.

The work input required by the pump is:

$$\dot{W}_{pump} = \dot{m} \cdot (h_2 - h_1)$$

Equation 6. Work power required in the pump.

Finally, the thermal efficiency of the ORC is defined on the basis of the first law of thermodynamics as the ratio of the net power output to the heat addition.

$$\eta_{thm} = \frac{W_{turbine} - W_{pump}}{Q_{evaporator}}$$

Equation 7. Thermal efficiency of the Organic Rankine Cycle.

For practical operation, the ORC has many parameters that have positive or negative effects on the ORC performance and that need to be modified together, involving a multi-dimensional surface on which an optimum could be found. In *section 3. Simulation and selection of the cycle main parameters*, the procedure followed to find the most suitable parameters for the ORC cycle is explained in order to achieve the objective of finding the optimum cycle to exploit the most frequent waste heat sources in the industry.

2. Waste heat data and market analysis in Europe

2.1. Waste heat data in Europe

The European Union (EU) is nowadays accountable for 11,6% of the world final energy consumptions (9.425 MTOEs in 2014) and for 10,8% of the world final CO_2 emissions (33,3 $GtCO_2$ in 2014). Within this framework, industry is responsible for the 25,9% of the final energy consumptions and for the 47,7% of the CO_2 emissions. The European Union has always been at the forefront of awareness and involvement for the depletion of current environmental issues. Indeed, present greenhouse gas emissions have been lowered by 22,9% compared to those in 1990. Going even further, one of the crucial EU targets for 2030 is the reduction of at least 40% with respect to the same reference year (1990) [24].

To accomplish this challenging objective, increasing the utilization not only of renewable energies but also of waste heat sources are unquestionably interesting directions to pursue. According to Panayiotou et al. [24] the waste heat recovery market is projected to reach $53,12 billion by the end of 2018, in which the European market is the most predominant: in 2012 it accounted for 38% of the global heat recovery equipment market. Moreover, it is also expected that the Asia-Pacific area will experience the highest growth rate in the following five years, with an estimated value of 9,7% per year and with the notable fact of China and India acquiring the highest number of installations based on heat recovery units.

The largest amounts of waste heat in industries are usually found in food, tobacco, pulp and paper, basic metals, chemical industry, and non-metallic minerals [25]. For these projections to materialize, and for the European industry to profit from these progresses, technological enhancements and innovations, aimed at improving the energy efficiency of heat recovery equipment and reducing costs, should be undertaken. Within this framework there are different technologies available to take advantage of the waste heat potential.

However, it is likewise essential to consider that temperature is one of the most important criteria when studying the feasibility of recovery deriving from waste heat sources. Some processes with lower temperature may not be a useful source directly, but the heat could be upgraded in case it is found a potential advantage on it. Typically, high temperature waste heat has more potential to be reused (namely operating with the classic Rankine cycle).

Figure 6 shows the distribution of high (temperature above 400 °C), medium (100 – 400 °C) and low temperature (below 100 °C) applications in different sectors in Germany for 2005 [26]. High temperature waste heat holds a large share of the processes in the metal manufacture and mineral processing sectors. On the other hand, the food and tobacco industry has only negligible amounts of high temperature heat demand.

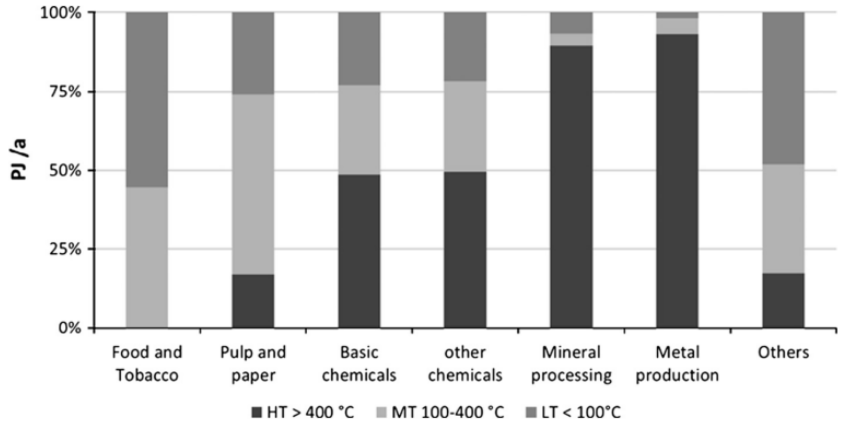

Figure 6. Process heat demand by temperature: high (HT), medium (MT) and low (LT) of different sectors, figure based on data from [26].

The present work only focuses on the medium range temperatures (between 100 and 400 ºC). Looking at the medium temperatures distribution in the graph, the main industry sectors of interest would be food and tobacco or pulp and paper. The main reason is that above 400 ºC the classic Rankine cycle operating with water is plausible, but below that value the use of a different type of working fluid is required in order to achieve better efficiencies. In addition, technology has not been developed enough to reach good performances from the heat sources at temperatures under 100 ºC.

Therefore, under these conditions, the main purpose of this work is determining the principal parameters of the organic Rankine cycle to convert into electricity a waste heat source at the medium temperatures. A more detailed picture of possible waste heat sources at temperatures between 100 and 400 ºC is given in *Table 2*. Here exhaust gas temperatures of different processes are given.

Industry	Process	Working temperature (ºC)
Food and beverages	Cooking	110 – 115 ºC
	Sterilizing	140 – 150 ºC
Textile	Drying	75 – 250 ºC
	Dyeing	100 – 160 ºC
	Steaming	100 – 130 ºC
Chemical	Distilling	110 – 300 ºC
	Other chemical processes	120 – 180 ºC
Paper industry	Pulp and paper drying	95 – 120 ºC
General	Finishing soaking pit reheat furnace	200 – 600 ºC
	Blast furnace stoves	250 – 300 ºC
	Drying and baking ovens	230 – 590 ºC
	Steam boiler exhaust	230 – 480 ºC
	Glass melting	160 – 200 ºC
	Conventional hot water boiler	60 – 230 ºC

Table 2. Exhaust gas temperatures of different processes, table based on data from [27].

2.2. Market analysis in the use of waste heat in Europe

Bearing in mind this huge amount of potentially profitable waste heat and that one of the most challenging objectives followed by the European energy strategies is reducing the quantity of primary energy consumed as well as the environmental concerns, a comprehensive research through the different waste heat sources in Europe was conducted.

When trying to find specific information about the amount of non-performed waste heat, its range of temperature and other valuable streams' data, it was found that not in many countries this information is collected. Indeed, although in several of these countries the energy strategies for the future years are based on the utilization of waste heat to improve the environmental issues, there are not precise data available in order to determine with accuracy this potential.

For instance, in Spain there are existing tools created with the aim of estimating the amount of residual heat in each area of the country, as it can be seen in Figure 7 [28]. This heat map displays the number of companies, within each region, that could offer residual heat. The colours represent the range of waste heat in terms of energy pro year, with the colour red representing the biggest providers of potential waste heat. Getting closer in a specific area, the map provides the information of each enterprise. However, this information is a rough estimate and without any accurate data about the sources (i.e. temperature or heat carrier).

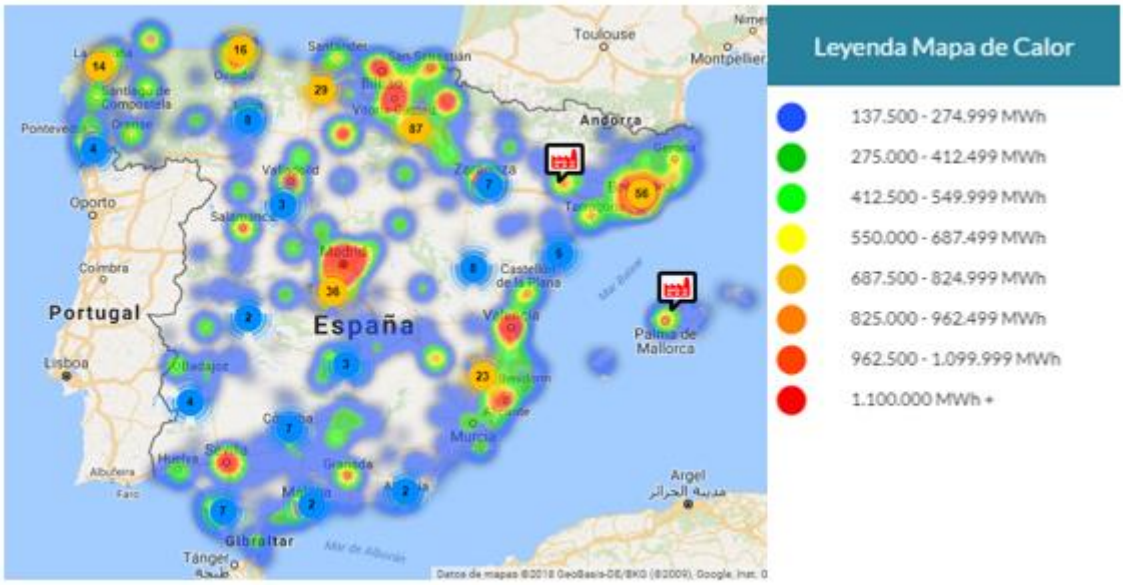

Figure 7. Map with the waste heat offer in Spain [28].

Even beyond, some attempts for assembling specific data from various companies, and studying some realistic circumstances, were intended. Nevertheless, it was found that none of them gathered this kind of information or that it was demanding to obtain some other parameters so that the information of interest could have been deduced. Thus, it was not possible to expand the analysis in this way. Among the reasons various of these companies explained, the ones that highlight are that the current regulations do not require collecting the amount of waste heat

and the fact that in most of the cases companies understand this residual heat as a waste and not as a potential profitable source.

Hence, the first limitation detected in this research was that in most of the European countries there is not a specific database which compiles information of the potentially recoverable waste heat. As an exception, Germany was the European country with more detailed data regarding this task. More specifically, the regions Saxony and Bavaria have their own heat maps (see *Figure 8* and *Figure 9*) [29] [30] similar to the Spanish.

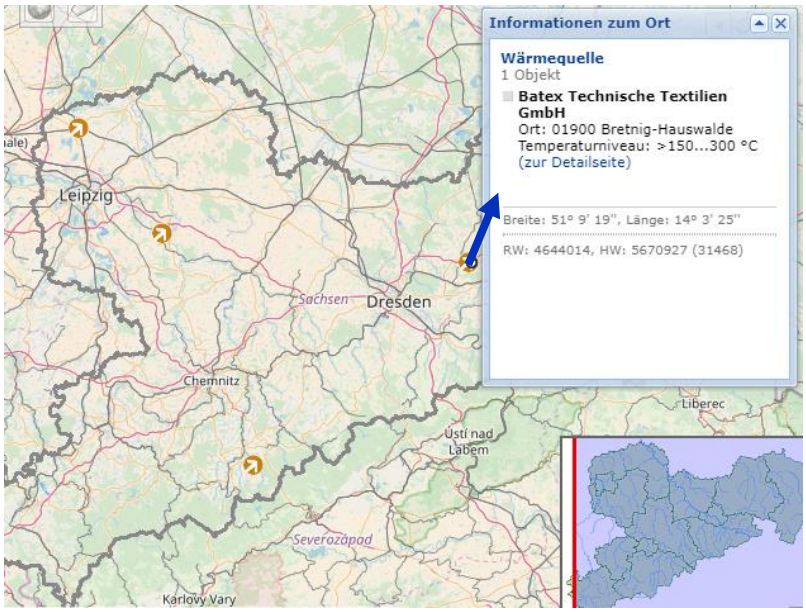

Figure 8. Saxony heat map for temperatures 150 – 300 ºC [29].

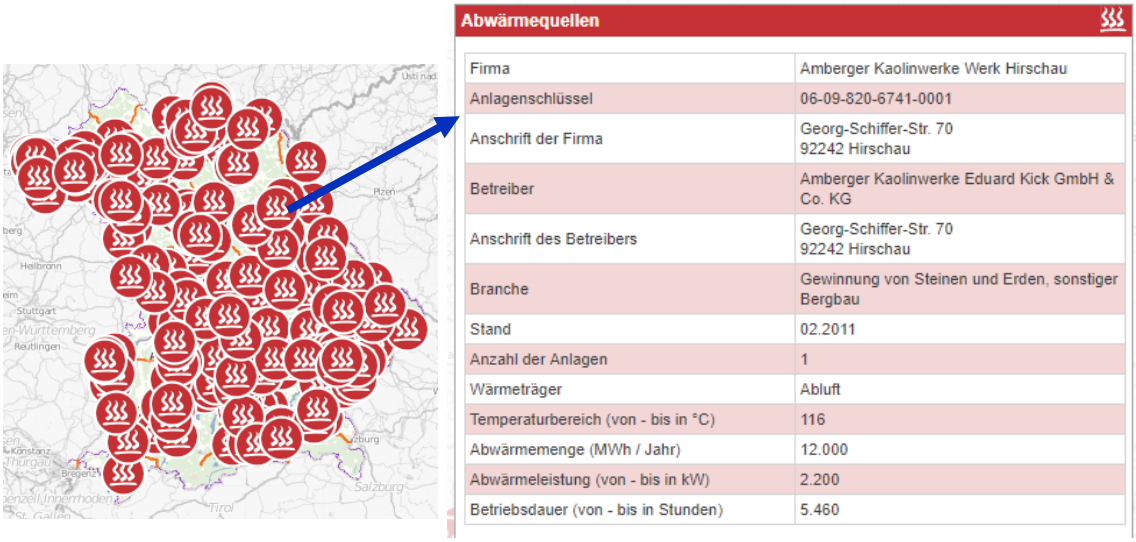

Figure 9. Bavaria heat map for temperatures 100 – 400 ºC [30].

These maps are more detailed than the Spanish one and the information contained among the three of them is compared in *Table 3*. First of all, basing the market analysis on the Spanish heat map was discarded due to its lack of temperature range, one of the most crucial criteria needed. Bearing in mind this table, the heat map which provides a more accurate and valuable information is the one from Bavaria. In addition, within Saxony map only 7 companies offer

waste heat at temperatures between 100 and 300 ºC (above 300 ºC all the manufactures are grouped). For these reasons, the analysis was performed with Bavaria map, not only for its more detailed information but also due to it provides a bigger sample. After the analysis was concluded, the middle of the market was established as the input conditions at the evaporator, enabling its conversion into electricity.

Information	Heat maps which include it
Temperature level	Saxony, Bavaria
Energy pro year	Saxony, Bavaria, Spain
Power	Bavaria
Heat carrier	Bavaria
Industrial sector	Saxony, Bavaria
Name of the company	Saxony, Bavaria
Operation time	Bavaria

Table 3. Information included in the three heat maps analysed.

Filtering in Bavaria heat map the companies that offer heat sources at temperatures between 100 and 400 ºC, 173 valid data were obtained. On the other hand, if the filter is set for temperatures above 400 ºC, only 16 results appear. This proves that the low-grade sources availability is broad and higher than the high-grade, and consequently that they are a great recovery potential with technologies such as organic Rankine cycle.

Figure 10 shows the distribution in temperature level of the heat sources in Bavaria. More than the 80% of the companies reject heat at temperatures below 200 ºC (30,4% at 100 - 150 ºC and 50,9% at 151 - 200 ºC). Then, at first sight, it seems that the most appealing temperature level to work with would be within this range.

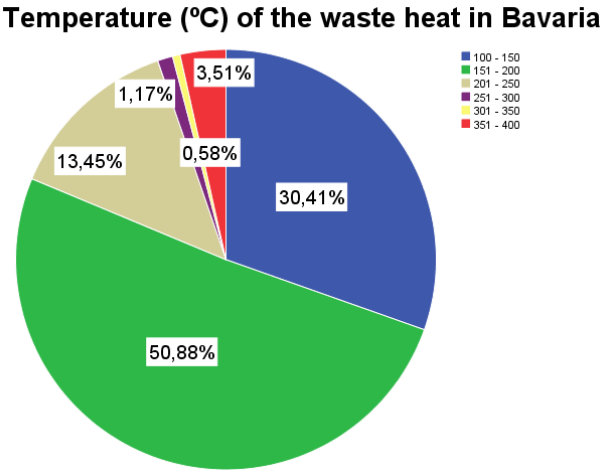

Figure 10. Temperature (ºC) of the waste heat from Bavaria heat map.

With the aim of determining which temperature offers the biggest potential for its recovery, *Figure 11* and *Figure 12* were analysed. In the first one it is possible to understand that the major amount of energy results from the lowest range of temperature (between 100 and 150 ºC). For

this reason, the temperature chosen for the heat flow provided at the evaporator of the system should lie between 100 and 150 ºC.

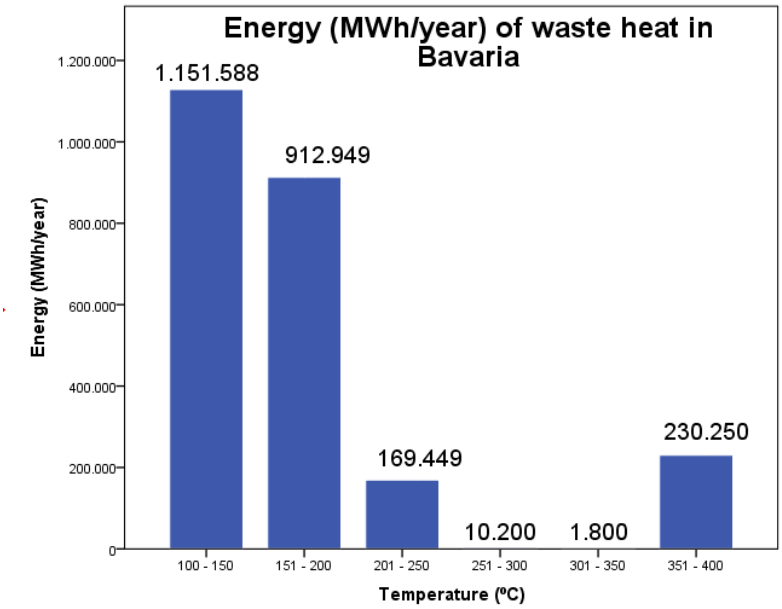

Figure 11. Energy (MWh/year) of waste heat for each range of temperature in Bavaria.

Another essential parameter to determine is the power provided by the heat source. Therefore, in *Figure 12* it is represented the frequency of each power value for the heat sources gathered in Bavaria map at the temperature range of 100 – 150 ºC. The most prevalent values are those of lowest power, under 400 kW. Thus, the power selected as the middle of the market for the evaporator supply is 200 kW.

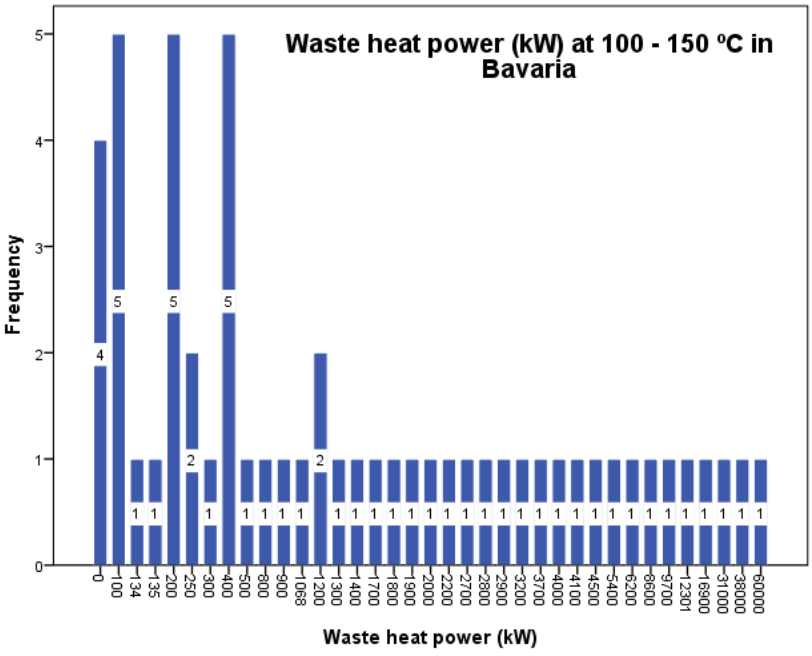

Figure 12. Waste heat power (kW) at 100 - 150 ºC in Bavaria.

The heat carrier distribution is presented in *Figure 13*. Looking at this chart, it is clear that exhaust air is the most common fluid, involving more than the 91% of the companies. Therefore, the heat carrier chosen for the evaporator in the model designed should be air.

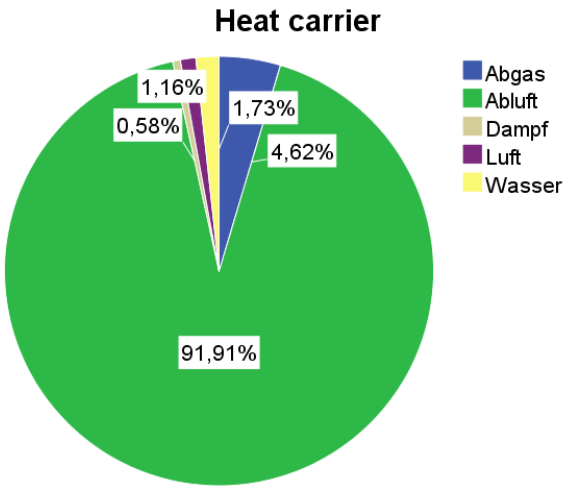

Figure 13. Heat carrier of the waste heat from the Bavaria heat map.

In conclusion, after these discussions were completed, the middle of the market deduced in terms of the waste heat offered by the industry is summarize in *Table 4*. These parameters will be determined as the input for the ORC model in Ebsilon. In other words, the heat exchanger working as evaporator will receive an air flow at 100 °C with 200 kW of heat power.

Temperature	100 °C
Power supply	200 kW
Heat carrier	Air

Table 4. Conclusions of the market analysis in the waste heat in Europe.

3. Simulation and selection of the cycle main parameters

3.1 Considerations in the fluid selection

One of the most important tasks that must be considered for a high system performance is the selection of the working fluid and its operation conditions. Due to it affects the efficiency of the cycle, the sizes of the system components, the design of expansion machine, the system stability, safety and environmental concerns, the selection of working fluids is crucial, not only for the ORC system performance but also for its economy. Different from the features of other thermodynamic cycles, such as compression refrigeration cycle (working conditions are determined) and Kalina cycle (working fluid composition is set although mass fractions vary), working fluid selection in ORC system is a more complicated task owing, basically, to the following two reasons [1]:

- The working conditions and heat source types of ORC vary widely depending on the manufactures offer.
- Except for some substances whose critical temperatures are too low or too high, hundreds of substances can be used as working fluid candidates of ORC, including hydrocarbons, aromatic hydrocarbons, ethers, perfluorocarbons, CFCs, alcohols, siloxanes and inorganics (which should not inherently be ORC candidates but due to the similarity with organics are included), etc.

Possible working fluids useful in organic Rankine cycle power systems are almost countless. Basically, good thermodynamic properties would result in high efficiency and low-cost systems. Furthermore, there are additional characteristics required in the selection of a suitable working fluid like: low toxicity, controllable flammability characteristics and explosion risk, good material compatibility and fluid stability limits, among others.

A substance may be toxic if it is ingested, inhaled or absorbed through the skin. Regarding this concern, the least toxic fluids are the refrigerants. The flammability hazard posed by each of the fluids is generally possible to be controlled. For this purpose, special vapor and fire detection equipment as well as suppression systems may be required for those fluids exhibiting the greatest potential hazard, involving some additional tasks and extra costs. Moreover, the fluid should be noncorrosive to common engineering materials, so that it does not dictate the use of more expensive materials, reducing the economic feasibility of the system. Finally, it is significant to consider that each fluid has its specific range of applicability up to the maximum limit of the stability temperature range without suffering significant decomposition [19].

Several analyses studying the influence of working fluids on the system efficiency were reported in the literature (see *heading 1.1.* in this document). Attempts were made to examine different types of working fluids and their effect on system efficiency by equation of state or correlation based on experimental data. Nevertheless, these analyses are difficult to apply directly since their results may lack of intuitive explanation and simple expressions.

3.1.1. Working fluids' category and their thermodynamic and physical properties

a) Working fluids' category

The working fluids could be categorized according to the saturation vapor curve, which is one of the most crucial characteristics of the working fluid in an ORC. This property affects the fluid applicability, cycle efficiency, and definition of related equipment in a power generation system. In some papers (for instance [8] [18]), the parameter ξ, defined in *Equation 8,* is used to express how "dry" or "wet" a fluid is:

$$\xi = ds/dT$$

Equation 8. Measure of the "dryness" or "wetness" of a working fluid [8].

As shown in *Figure 14*, according to the slope of the temperature-entropy curve (dT/ds) in the temperature-entropy (T-s) diagram, there are generally three types of fluids:

- Dry fluids: which have positive slope ($\xi > 0$), and they are in general of high molecular numbers, such as R113 and Benzene.
- Wet fluids: which have negative slope ($\xi < 0$), and they are usually of low molecular members, such as water.
- Isentropic fluids: which have nearly vertical saturated vapor curve ($\xi \approx 0$), such as R11 and R12.

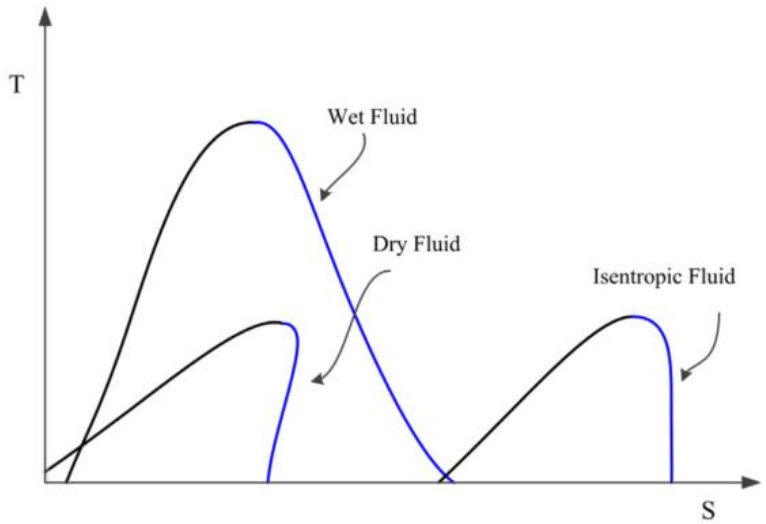

Figure 14. Classification of the working fluids according to the slope of the saturation curve in T-s diagram [31].

Due to the negative slope of the saturation vapor curve for a wet fluid, outlet stream of the turbine typically contains saturated liquid. Presence of liquid inside turbine may damage turbine blades and it also decreases the isentropic efficiency of the device. Typically, the minimum steam fraction at the outlet of a turbine is kept above 85%. To satisfy this minimum dryness fraction at the outlet of the turbine, the wet working fluid should be superheated at the inlet of

the turbine, while isentropic and dry fluids do not need overheating, thereby avoiding the problems arising from liquid droplets on the expander blades.

This means that dry or isentropic fluids tend to be more adequate for ORC systems. It should be also taken into account that if the fluid is "too dry", the expanded vapor will leave the turbine with great "superheat", which is a waste and additional load to the cooling device. In this case, a regenerator is commonly used (see *Figure 5*) to reclaim these exhaust vapor and rise the cycle efficiency; however, it would as well increase the system's initial investment and complexity.

b) Classification under the structural point of view

Furthermore, from the structural point of view and type of atoms in the fluid molecule, the ORC working fluids can be categorized under seven main classes [1]:

1. Hydrocarbons (HCs)

Including linear (n-butane, n-pentane), branched (isobutane, isopentane), and aromatic hydrocarbons (toluene, benzene) have:

- Desirable thermodynamic characteristics
- Flammability concerns

Ethane	Propene	Propane	Cyclopropane	Propyne	Isobutane
Isobutane	Isobutene	N-butane	Neopentane	Isopentane	N-pentane
Isohexane	N-hexane	N-heptane	Cyclohexane	N-octane	N-nonane
N-decane	N-dodecane	Benzene	Toluene	p-Xylene	Ethylbenzene
N-propylbenzene	N-butylbenzene				

2. Perfluorocarbons (PCFs)

The fully fluorinatedhydrocarbons which are/have:

- Extremely inert and stable
- Extreme molecular complexity
- Thermodynamically undesirable

Carbon-tetrafluoride (R14)	Hexafluoropane (R116)	Octafluoropropane (R218)
Perfluoro-N-oentane (PF5050)	Decafluorobutane (R-3-1-10)	Dodecafluoropentane (R-4-1-12)

3. Siloxanes

- Attractive for a mix of physical and thermal properties (low toxicity and flammability level, high molecular mass, prolonged use as high temperature heat carrier)
- They are often available as mixtures rather than as pure fluids
- Isobaric condensation and evaporation are not isothermal and exhibit a certain glide

Hexamethyldisiloxane (MM)	Octamethyltrisiloxane (MDM)	Decamethyltetrasiloxane (MD2M)
Dodecamethylpentasiloxane (MD3M)	Octamethylcyclotetrasiloxane (D4)	Decamethylcyclopentasiloxane (D5)

4. Partially fluoro-substituted straight chain hydrocarbons

- Some of them have zero ODP (Ozone Depletion Potential)
- Many have considerable potential interest

Hydrofluorocarbons (HFCs)					
R23	R32	R41	R125	R134a	R143a
R152a	R227ea	R236fa	R236ea	R245fa	R245ca
RC318	R338mccq	R365mfc			
Chlorofluorocarbons (CFCs)					
R11	R12	R113	R114	R115	
Hydrochlorofluorocarbons (HCFCs)					
R21	R22	R123	R124	R141b	R142b

5. Ethers and fluorinated ethers

Are characterized for:

- Flammability and toxicity issues
- Thermodynamically undesirable

Fluorinated ethers				
RE125	RE134	RE245	RE245mc	RE347mcc
Ethers				
RE170	R610			

6. Alcohols

Have:

- Flammability issues
- Soluble in water
- Thermodynamically undesirable

Methanol	Ethanol

7. Inorganics

- Extensive and inexpensive
- Small environmental impact
- Some operation problems

Ammonia (R717)	Water (R718)	Carbon dioxide (R744)

Even if the possibilities when choosing the appropriate working fluid for the ORC are nearly countless, and although it is feasible to use different mixtures of pure working fluids, within this work only pure alternatives will be considered. Due to working fluid selection is crucial for ORC system performance and economy, many researchers have developed working fluid screening. The screening method is by far the most used technique for fluid selection in the scientific literature: it consists in building steady-state simulation model of the ORC cycle and run it with different working fluids.

This procedure is the one followed throughout this work (explained with more detail in heading *3.3. Simulation in Ebsilon*). Looking at the previous classification, as a start point for the selection of the working fluids that will be screened, it could seem that the most interesting fluids to be evaluated are the ones gathered in the category *4. Partially fluoro-substituted straight chain hydrocarbons*.

c) The thermodynamic and physical properties

The performance of ORC systems strongly depends on working fluids' properties, which influence system efficiency, operating conditions, environmental impact and economic viability. The relationship between working fluid characteristics and the ORC typical economic and thermodynamic performance criteria, are discussed as follows from a theoretical and analytical point of view [1] [8]:

1) Vaporization latent heat

Chen et al. [8] found that when the heat source is waste heat, organic fluids with lower specific vaporization heat are preferred. Lower vaporization heat of the working fluid causes the heat transfer process in the evaporator to occur mainly at variable temperature. Therefore, the temperature profile of the working fluid better follows the temperature profile of the heating fluid in the evaporator. This means that the temperature difference between fluids in the heat exchanger is reduced as reflected in *Figure 15*, hence the irreversibility in the heat transfer process is decreased.

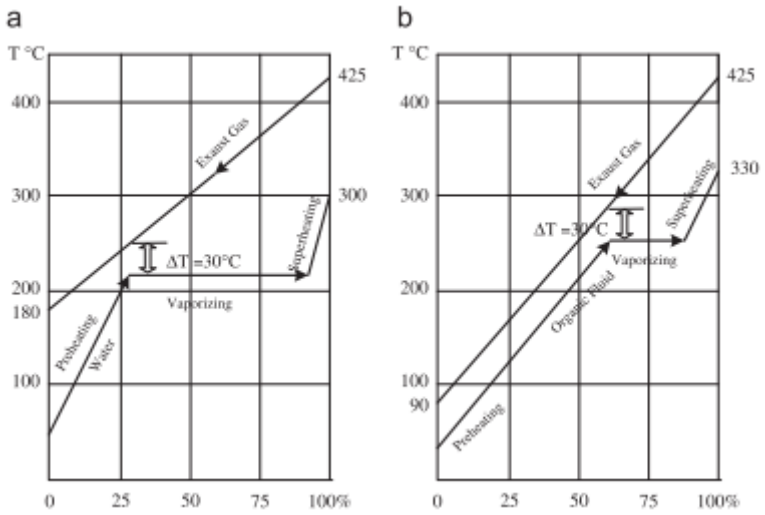

Figure 15. The effects of vaporization latent heat on the irreversibility in the heat transfer process: a) water b) organic fluid [1].

2) Density

High vapor density is of key importance, especially for fluids showing a very low condensing pressure (e. g. silicon oils). A low density leads to a higher volume flow rate so that the pressure drops in the heat exchangers are increased, and the size of the expander needs to be augmented. Additionally, this would have a significant effect on the cost of the system.

3) Liquid specific heat

Liquid specific heat should be low so that it could decrease the work consumed by pump and increase the work output indirectly.

4) Critical points

The condensation temperature is usually above 300K in order to reject heat to the ambient. Thus, fluids like methane with critical temperatures are far under 300K lie out of consideration due to the difficulty in condensing.

Additionally, the critical point of a working fluid, being the peak point of the fluid saturation line in a T-s diagram, indicates the proper operating temperature range for the working fluid. Another important thermodynamic property is the freezing point of the fluid, which must be below the lowest operating temperature in the cycle. The fluid must also work in an acceptable pressure range: very high pressure or excessive vacuum tend to impact the cost.

5) Boiling temperature

The boiling temperature is expected to be between 0 and 100 ^{o}C.

6) Molecular weight

Expansion work tends to be in inverse relation to molecular weight which means that turbines for heavy fluids tend to have a low peripheral speed and a small number of stages. In general, complex molecules are also heavy and this characterizes most organics.

7) Viscosity

A low viscosity both in the liquid and vapor phases is required to maintain low friction losses in the heat exchangers and pipes.

8) Conductivity

High conductivity is required to obtain a high heat transfer coefficient in the heat exchangers.

9) Stability of the fluid and compatibility with materials in contact

Unlike water, organic fluids usually suffer chemical deterioration and decomposition at high temperatures. The maximum operating temperature is therefore limited by the chemical stability of the working fluid. Additionally, the working fluid should be non-corrosive and compatible with engine materials and lubricating oil.

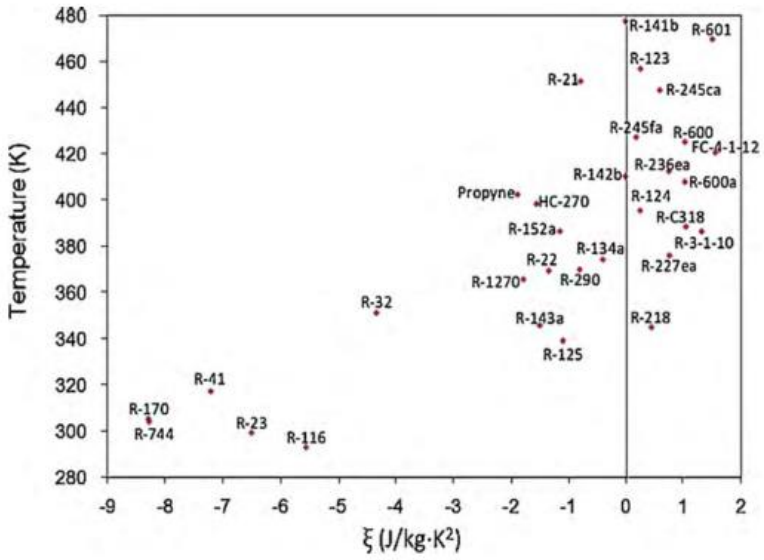

Figure 16. Possible ORC fluids in the T-ξ chart [8].

The first decision made for the fluid selection in the present work was that the working fluid for the ORC turbomachine should be "dry", ensuring that there are no droplets during the expansion in the turbine and avoiding the possibility of damage on its blades. In this context and looking at *Figure 16* (and to the previous classification), the fluids considered as feasible for the simulations in Ebsilon were:

R218 R227ea R236ea R245ca R245fa RC318 R600 R600a R601

Table 5, based on the data from [8], collects the main properties of this group of working fluids.

- Molecular mass (g/mol)
- Critical temperature (Tc – ºC)
- Critical pressure (Pc – Mpa)
- Latent heat of vaporization (kJ/kg)
- ξ (J/kg K^2)

Fluid	Name	Molecular formula	Molecular weight (g/mol)	Tc (ºC)	Pc (MPa)	Latent heat of vaporization (kJ/kg)	ξ (J/kg K^2)
R218	Octafluoropropane	C_3F_8	188,02	71,9	2,64	58,29	0,45
R227ea	1,1,1,2,3,3,3-Heptafluoropropane	C_3HF_7	170,03	101,8	2,93	97,14	0,76
R236ea	1,1,1,2,3,3-Hexafluoropropane	$C_3H_2F_6$	152,04	139,3	3,5	142,98	0,76
R245ca	1,1,2,2,3-Pentafluoropropane	$C_3H_3F_5$	134,05	174,4	3,93	188,64	0,60

R245fa	1,1,1,3,3-Pentafluoropropane	$C_3H_3F_5$	134,05	154,0	3,65	177,08	0,19
RC318	Octafluorocyclobutane	C_4F_8	200,03	115,2	2,78	93,95	1,05
R600	Butane	C_4H_{10}	58,12	152,0	3,8	336,82	1,03
R600a	Isobutane	C_4H_{10}	58,12	134,7	3,63	303,44	1,03
R601	Pentane	C_5H_{12}	72,15	196,6	3,37	349,00	1,51

Table 5. Physical properties for the screened working fluids, data collected from [8].

Paying attention to *Table 5*, the refrigerant R218 was the first one excluded from the study because of its critical temperature. This value is 71,9 ºC, almost 30 ºC below the heat source temperature (100 ºC). Therefore, the fluids which will be considered in the next step of the work, the environmental and safety concerns analysis, are:

R227ea R236ea R245ca R245fa RC318 R600 R600a R601

3.2.2. Environmental and safety properties

Generally, characteristics like non-corrosive, non-flammable, and non-toxic are expected for the working fluids. But they are not always practically satisfiable or critically necessary. Many substances, like R-601, are considered flammable but this is not a problem if there is no ignition source around. However, autoignition is a challenge, in particular for longer alkanes at temperatures above 200 ºC. Within this framework, the ASHRAE refrigerant safety classification is a good indicator of the fluid's level of danger [1].

For these reasons, in *Table 6* the safety and environmental data for these working fluids has been compiled [32]:

Safety data:

- *Occupational exposure limit (OEL),* measured in ppm v/v for an 8 (sometimes 10) hour day and 40 hours work week on a time-weighted average. It is the upper limit on the acceptable concentration of a hazardous substance. It is typically set by competent national authorities and enforced by legislation to protect occupational safety and health. They include the Threshold Limit Value (TLV) assigned by the American Conference of Governmental Industrial Hygienists (ACGIH9), Workplace Environmental Exposure Level (WEEL) by the American Industrial Hygiene Association (AIHA), Recommended Exposure Limit (REL) by the U.S National Institute for Occupational Safety and Health (NIOSH), maximale Arbeitsplatz-Konzentration (MAK values) by Deutsche Forschungsgemeinschaft (DFG), OEL by the Japan Society for Occupational Health (JSOH) and Permissible Exposure Limit (PEL) by the U.S.

- *Lower Flammability Limit (LFL),* measured in % concentration in ambient air. The values are those determined in accordance with ASHRAE Standard 34.

- *Safety classification*, if assigned, in accordance with ASHRAE 34. As shown in *Figure 17*, the leading letters A and B mean "lower" and "higher" toxicity, respectively, based on occupational exposure limits like TLV (Threshold Limit Value) and TWA (Time Weighted Average).
    - *Class A: TLV/TWA 400 ppm or higher*
    - Class B: TLV/TWA 399 ppm or lower

  The numbers 1, 2 and 3 indicate "no flame propagation", "lower flammability" and "higher flammability", respectively, at specified test conditions predicated on both LFL and heat of combustion.
    - Class 1: "no flame propagation"
    - Class 2: "lower flammability"
    - Class 3: "higher flammability"

  For instance, a refrigerant "A1" is one of the safest refrigerants. On the other hand, "B3" means that the fluid is the most dangerous type of refrigerant to use as a working fluid in the ORC.

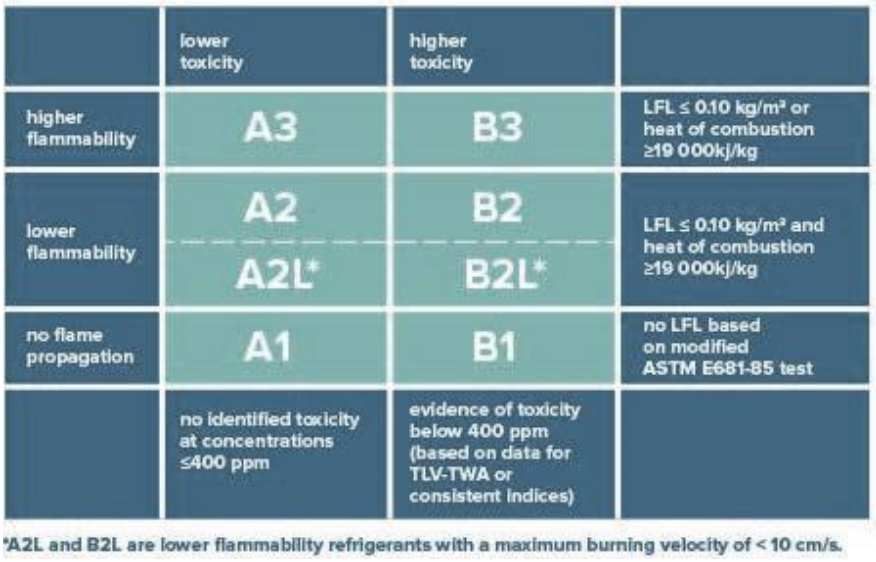

Figure 17. ASHRAE 34 Safety Classification [33].

Environmental data:

As to the environmental aspects, the main concerns include the Ozone Depletion Potential (ODP), Global Warming Potential (GWP) and the Atmospheric Lifetime (ALT). The ODP and GWP represent substance's potential to contribute to ozone degradation and global warming. Due to environmental concerns, some working fluids have been phased out, such as R11, R12, R113, R114, and R115, while some others are being phased out in 2020 or 2030 (such as R21, R22, R123, R124, R141b and R142b). In the working fluids primary selection those phased-out substances may be not included. The most important criteria are:

- *Atmospheric lifetime (ATL)* in years.
- *Ozone Depletion Potential (ODP)* relative to R11 (a CFC). ODPs indicate the relative ability of refrigerants (and other chemicals) to destroy stratospheric ozone. The values

included reflect the latest scientific consensus data as adopted in the World Meteorological Organization (WMO) Scientific Assessment (2010).

- *Global Warming Potential (GWP)* relative to CO_2 for 100 years, based on the values reported in the Intergovernmental Panel on Climate Change (IPCC) Fourth Assessment Report in 2007 and as updated in the WMO (2010) Scientific Assessment.

Table 6 contains the environmental and safety data for the group of fluids resulted from the first step: the analysis of physical properties.

Fluid	Safety data			Environmental data		
	OEL (ppmv)	LFL (%)	Std 34 safety group (ASHRAE)	ATL (years)	ODP	GWP (100 years)
R227ea	1000	none	A1	38,9	0,000	3580
R236ea	1000	none		11,0	0,000	1410
R245ca		7,1		6,5	0,000	726
R245fa	300	none	B1	7,7	0,000	1050
RC318	1000	none	A1	3200	0,000	10300
R600	1000	2,0	A3	0,018	0,000	20
R600a	1000	1,6	A3	0,016	0,000	20
R601	600	1,2	A3	0,009	0,000	20

Table 6. Safety and environmental data for the screened working fluids, in the basis of [32].

In *Figure 18* the evolution in the use of the refrigerants through the history can be assessed. This evolution shows that the greatest effort made during the latest research lies in the efficient use of working fluids with lower ODP (Ozone Depletion Potential) as well as decreasing GWP (Global Warming Potential).

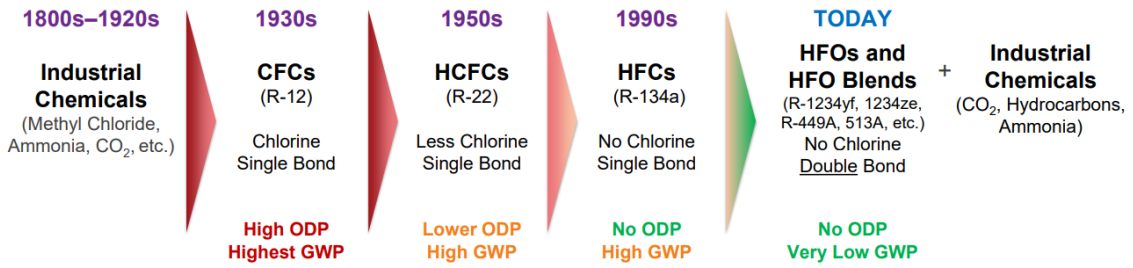

Figure 18. History of refrigerants transition [34].

Looking at the different safety and environmental parameters, some prior conclusions could be asserted:

- Refrigerants R227ea and RC318 are included in the safest category according to ASHRAE Standard 34.
- R245ca was discarded due to its highest flammability. Even if the hydrocarbons (R600, R600a and R601) have lower LFL, they were as well excluded so that it is not necessary to have any kind of consideration for a special design regarding the equipment.

- The main advantage of R245fa is its lowest OEL, comparing to the rest of the working fluids.
- Unlike the hydrocarbons, the main disadvantage regarding the rest of the fluids (all of them are HFCs) is their still large Global Warming Potential (GWP), even if it is lower than CFCs for instance (see *Figure 18*).

In conclusion, the fluids that were screened in the simulations to find the optimal cycle conditions are:

R227ea R236ea R245fa RC318

3.3. Simulation in Ebsilon

Taking into account the conclusions deduced from the first preliminary analysis about the most notable physical properties as well as the environmental and safety concerns, the fluids considered as appropriate to be studied with the software Ebsilon were the following:

R227ea R236ea R245fa RC318

The model designed in Ebsilon is presented in *Figure 19*. It consists on the main elements of the organic Rankine cycle (ORC): one heat exchanger working as an evaporator, a turbine, an additional heat exchanger working as the condenser and a pump. Throughout this document the four different states of the cycle will be referred as numbers (from 1 to 4), in order to address easily the conditions at the inlet and outlet of each one of the components.

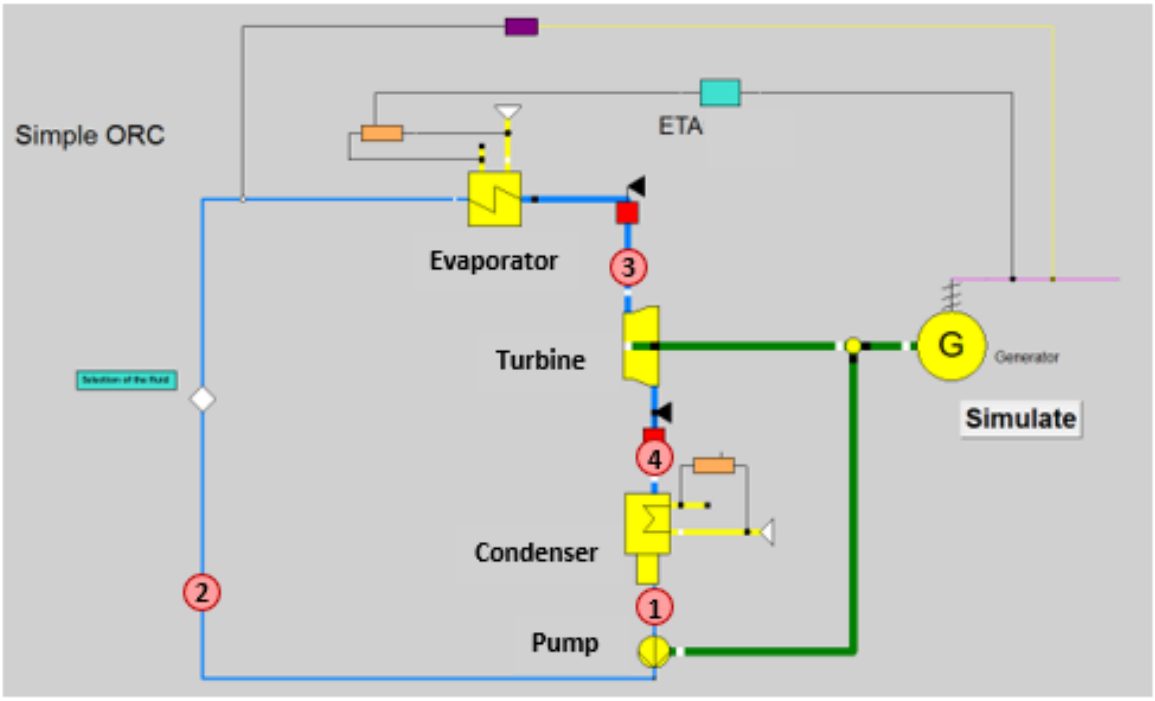

Figure 19. Components of the model in Ebsilon.

Regarding the main parameters of the different devices, this software defines predetermined values which were considered as realistic and appropriate for the first design. For that reason, the unique inner parameters modified in the model were the isentropic efficiencies of the turbine and the pump. Specifically, these parameters were adjusted with the values:

	Isentropic efficiency
Turbine	0,75
Pump	0,6

Table 7. Isentropic efficiencies for the turbine and the pump.

The aim of this study is establishing the most suitable conditions for the ORC and system performance, on the basis of the waste heat offer deduced from the market analysis. This market analysis is rooted in the waste heat necessities of different companies (see heading *2.2. Market analysis in the use of waste heat in Europe*). However not only the heat sources should be considered, it is also crucial paying attention to the cold sources available in those companies. Accordingly, in order to be independent of the cold sources availability within the company, the cycle was designed with an air cooler device that provides an air flow with 15 ^{o}C for the condenser.

3.3.1. Simulations with a controller to set the electric net power

With the purpose of studying the maximum electrical net power possible for each of the screened fluids, a controller was established. The procedure followed consisted on setting a specific value for the electric power as target variable. After an amount of iterations, the controller finds the adequate mass flow of the working fluid, the corrected variable. In order to conduct this analysis, the electric power together with the pressure levels were modified with the help of an Excel file linked to the model in Ebsilon software. For each attempt of a fixed net electric power, different pressure levels at the inlet and outlet of the turbine were tested:

- The pressure level at the outlet of the turbine begins as the pressure for a condensing temperature of 18 ^{o}C, and it is increased in 0,1 bar for each attempt.
- The pressure level at the inlet of the turbine varies starting with the pressure level resulted from the evaporating temperature equal to 100 ^{o}C and it is reduced in 0,1 bar for each attempt until the pressure is nearly the condensing fixed pressure.

For example, if the organic fluid chosen is R236ea:

Attempt	$W_{electric}$ (kW)	P_4 (bar)	P_3 (bar)
1	7,8	1,64	15,75
2	7,8	1,64	15,65
…	…	…	…
	7,8	1,74	15,75
	7,8	1,74	15,65
	…	…	…

Table 8. Example of the procedure for the simulations with a controller in Ebsilon.

The viable results found after this study are summarized in *Table 9*. This means that for these attempts the outcome obtained with Ebsilon turned out to be "Success" while in the rest of the iterations it resulted in "Error in Calculation". The attempts carried out with R227ea as working fluid only performed powers under 7,5 kW, and therefore they have not been included in *Table 9*.

Fluid	Electric power (kW)	P_4 (bar)	P_3 (bar)	ETA	T_4 (°C)	m (kg/s)	T_3 (°C)	T_{ev} (°C)
R236ea	7,8	1,74	6,35	0,0770	20,25	0,5414	61,95	61,94
	7,8	1,74	6,25	0,0762	20,25	0,5480	61,51	61,35
	7,8	1,74	6,15	0,0753	20,25	0,5555	60,86	60,75
RC318	7,7	2,64	10,51	0,0783	19,83	0,7170	69,80	69,28
	7,7	2,64	10,41	0,0778	19,83	0,7188	70,04	68,87
R245fa	7,5	1,2	5,44	0,0857	19,42	0,3428	91,97	65,79
	7,5	1,2	5,34	0,0848	19,42	0,3468	91,59	65,12
	7,5	1,2	5,24	0,0839	19,42	0,3511	91,17	64,43
	7,5	1,2	5,14	0,0829	19,42	0,3555	90,72	63,74

Table 9. Viable cycles for fluids studied: R236ea, RC318 and R245fa.

*ETA refers to *Equation 7*: $\eta_{thm} = \frac{W_{turbine} - W_{pump}}{Q_{evaporator}}$ but also considering the efficiency of the generator which transforms the mechanical work into electricity.

From this table it can be regarded that when the electric power and the lower pressure level are fixed, the higher the pressure at the entrance of the expansion device is, the higher the thermal efficiency results. This inference can easily be explained by the fact that the work power in the expansion is higher, so that the efficiency is raised (*Equation 7*). Hence, under this situation for each working fluid, the optimal cycle is the one, among the feasible cycles, with the highest pressure at the inlet of the turbine.

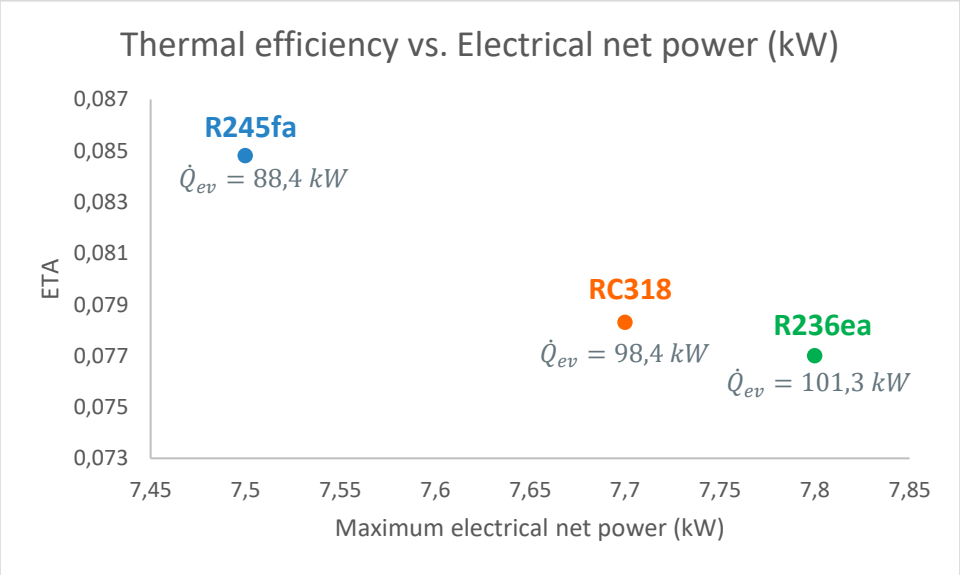

Figure 20. Thermal efficiency vs. Electrical net power (kW) for the fluids R245fa, RC318 and R236ea.

When comparing the optimum cycle within the different working fluids, it is found that the maximum electric net power possible varies between 7,5 kW for R245fa and 7,8 kW for R236ea.

It is also visible that the higher the electric power is, the lower the thermal efficiency becomes. These performances oscillate from 0,077 for R236ea and 0,0857 for R245fa, as can be observed in *Figure 20*. This reduction in the efficiency when the electric power increases is caused by the raising heat transferred in the evaporator: the growth of the heat is higher than the rise in the electric power. That means, according to *Equation 7*, the efficiency tends to be lower.

In *Figure 21*, the effect of the pressure at the inlet of the turbine on the working fluid mass flow is presented. This graph displays the fact that there are no big differences referring to the way the pressure affects the mass flow among the three working fluids. In other words, the slope is very similar for the three refrigerants. But more specifically, R236ea is the one more affected by the alteration of the highest pressure level, while RC318 is the least influenced.

An additional and remarkable fact is that even modifying the mass flow and the pressure at the inlet of the turbine (both parameters are related), it is possible to achieve the same electric power as a result of the cycle performance. This could be definitely useful in terms of the system's regulation, offering a range of possibilities. Although the efficiency decreases when rising the mass flow and reducing the pressure, this depletion is not significant (see *Table 9*). For that reason, in the succeeding graph, only the average efficiency is represented.

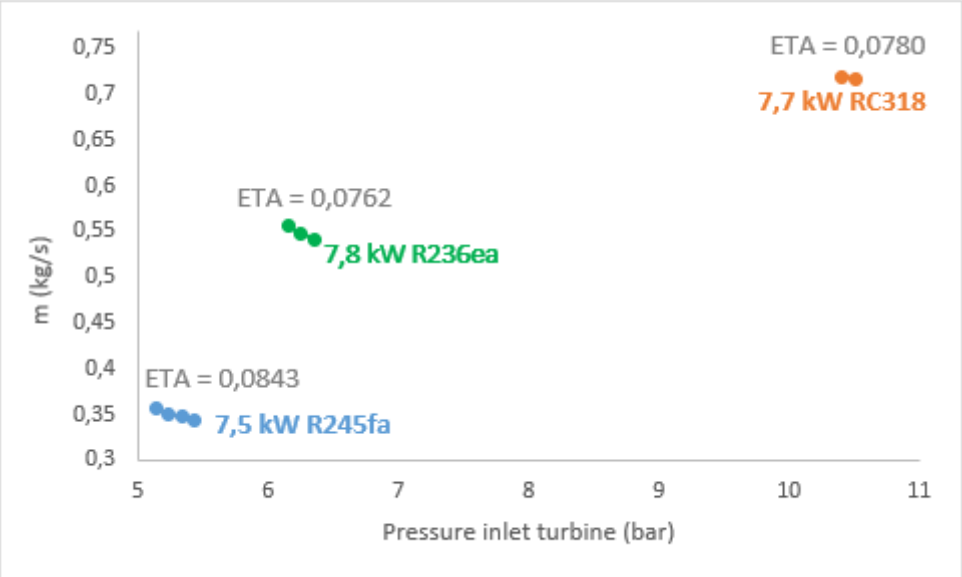

Figure 21. Mass flow (kg/s) vs. pressure at the inlet of the turbine (bar) for the maximum electric power (kW) within each fluid.

Hereunder, the main results of the three working fluids are collected, selecting as optimal cycle for each of them the one with highest efficiency and pressure at the inlet of the turbine as well as lowest mass flow (first row of each one in *Table 9*). The outcomes in Ebsilon and the T-s diagrams for each one of the cycles are featured below (note that the temperature levels of the air in the evaporator and the condenser are represented).

a) Best result for R245fa

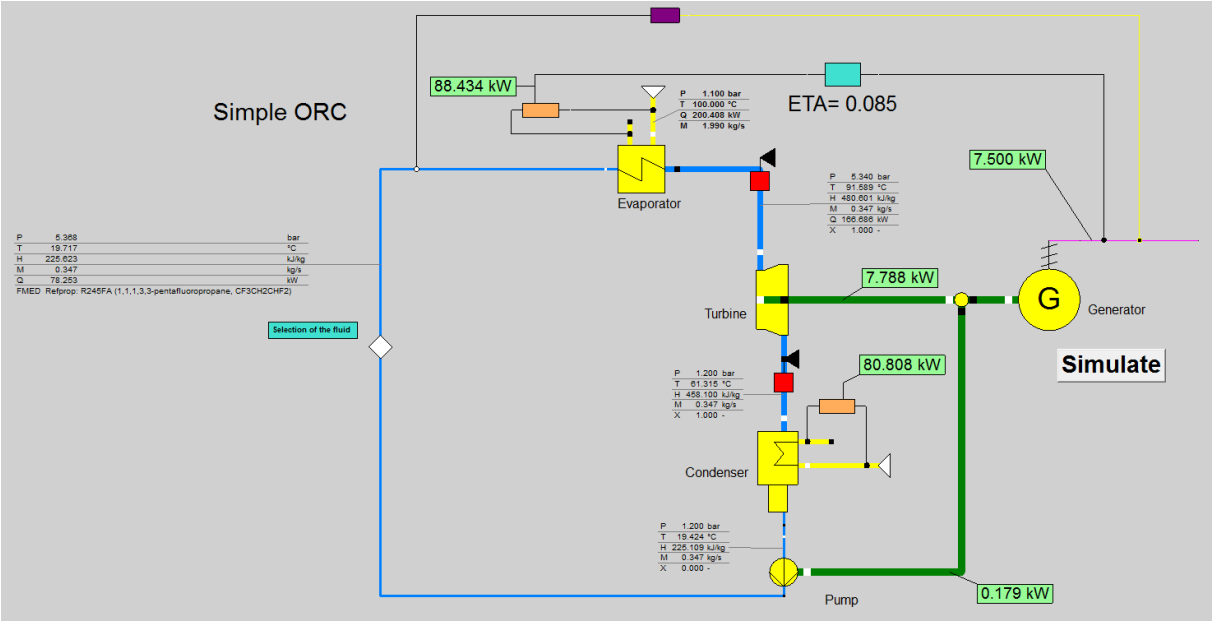

Figure 22. Model in Ebsilon for R245fa and 7,5 kW.

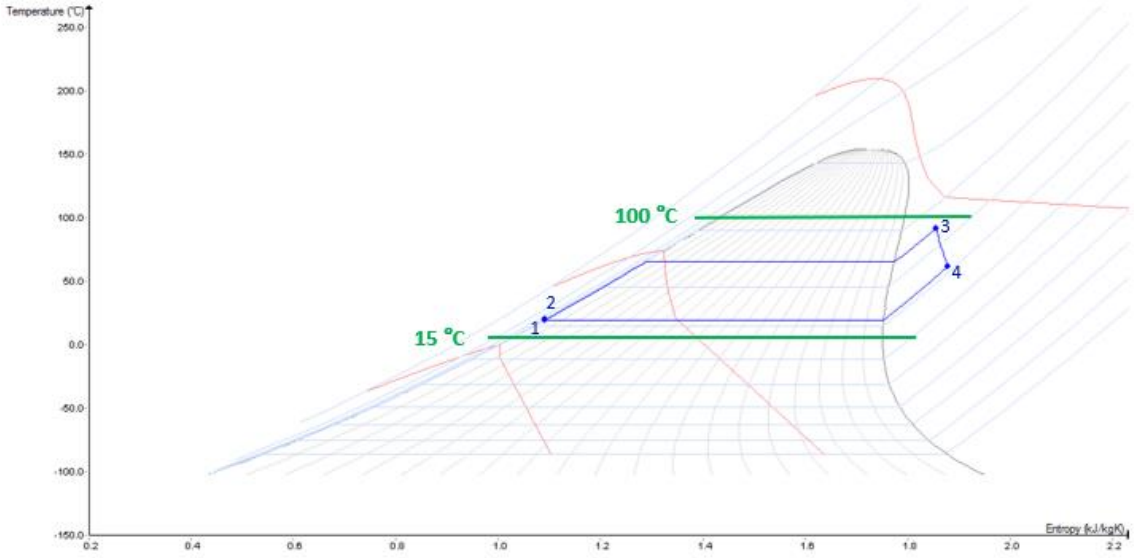

Figure 23. T-s diagram for R245fa and 7,5 kW.

The main outcomes are collected in the following tables:

$\dot{W}_{electric}\ (kW)$	7,5
$\dot{W}_{turbine}\ (kW)$	7,788
$\dot{W}_{pump}\ (kW)$	0,179
$\dot{Q}_{evaporator}\ (kW)$	88,434
$\dot{Q}_{condenser}\ (kW)$	80,808
Efficiency (ETA)	0,085

Table 10. Main results for R245fa.

Point	T (°C)	P (bar)	H (kJ/kg)	m (kg/s)
1	19,424	1,2	225,109	0,3428
2	19,717	5,368	225,623	
3	91,589	5,34	480,601	
4	61,315	1,2	458,100	

Table 11. Main parameters of R245fa cycle.

b) Best result for RC318

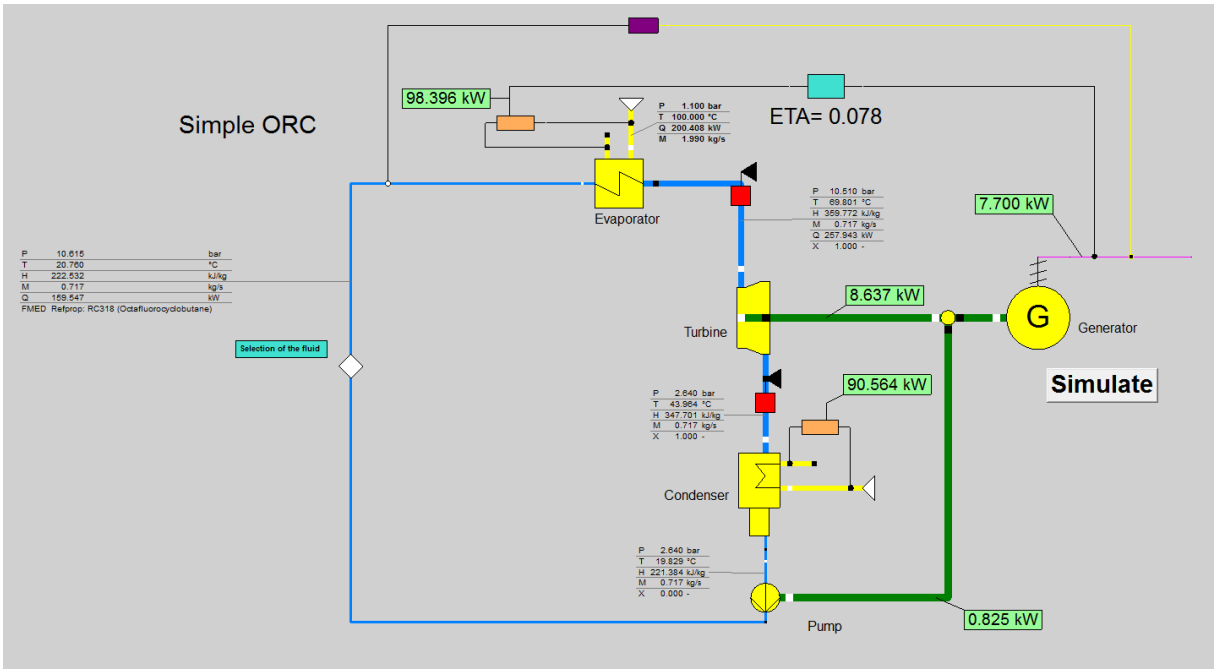

Figure 24. Model for RC318 and 7,7 kW.

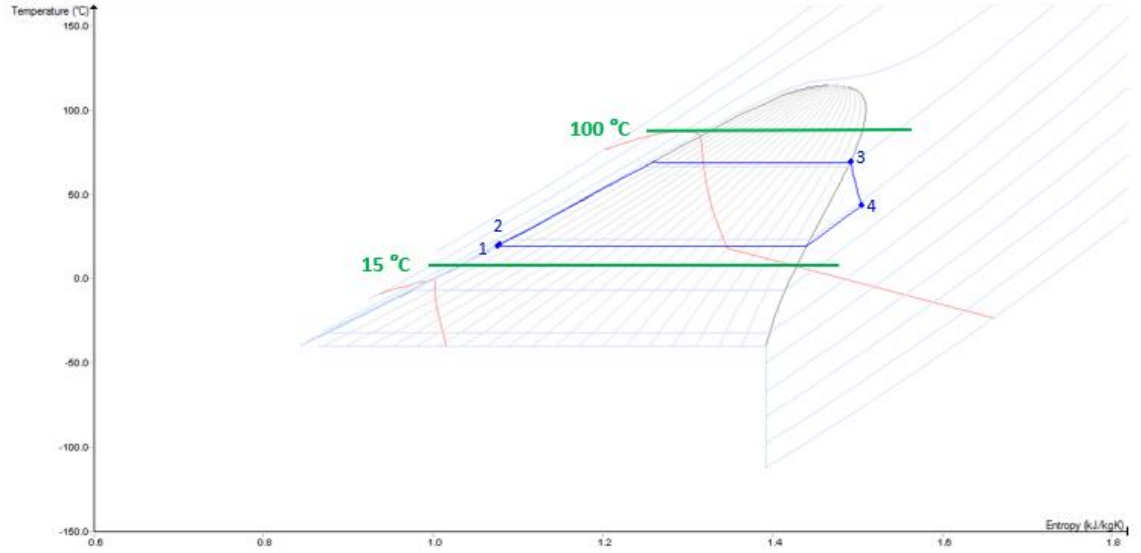

Figure 25. T-s diagram for RC318 and 7,7 kW.

$\dot{W}_{electric}\ (kW)$	7,7
$\dot{W}_{turbine}\ (kW)$	8,637
$\dot{W}_{pump}\ (kW)$	0,825
$\dot{Q}_{evaporator}\ (kW)$	98,396
$\dot{Q}_{condenser}\ (kW)$	90,564
Efficiency (ETA)	0,078

Table 12. Main results for RC318.

Point	T (°C)	P (bar)	H (kJ/kg)	m (kg/s)
1	19,829	2,640	221,384	0,717
2	20,760	10,615	222,532	
3	69,801	10,510	359,772	
4	43,964	2,640	347,701	

Table 13. Main parameters of RC318 cycle.

c) Best result for R236ea

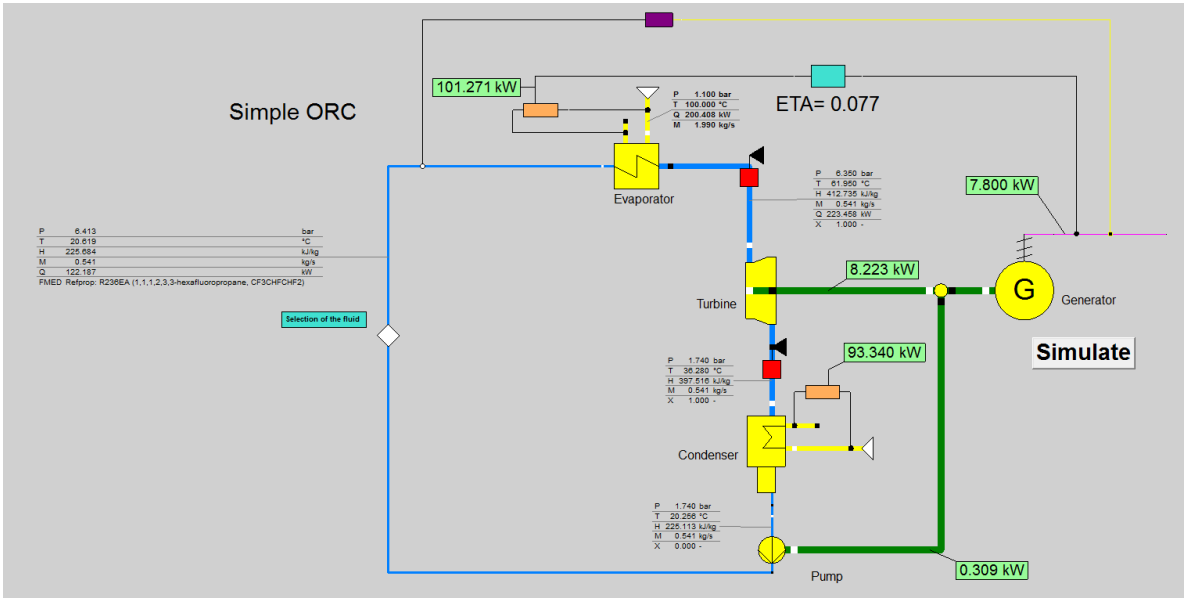

Figure 26. Model for R236ea and 7,8 kW.

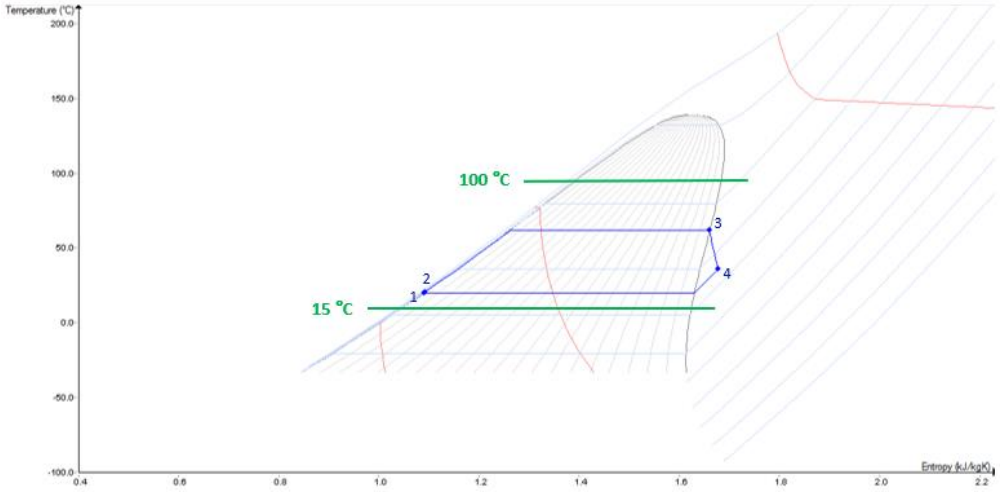

Figure 27. T-s diagram for R236ea and 7,8 kW.

$\dot{W}_{electric}\ (kW)$	7,8
$\dot{W}_{turbine}\ (kW)$	8,223
$\dot{W}_{pump}\ (kW)$	0,309
$\dot{Q}_{evaporator}\ (kW)$	101,271
$\dot{Q}_{condenser}\ (kW)$	93,340
Efficiency (ETA)	0,077

Table 14. Main results for R236ea.

Point	T (°C)	P (bar)	H (kJ/kg)	m (kg/s)
1	20,256	1,740	225,113	0,5414
2	20,619	6,413	225,684	
3	61,950	6,350	412,735	
4	36,280	1,740	357,516	

Table 15. Main parameters of R236ea cycle.

Figure 28 and *Figure 29* summarize the fundamental outcomes of the simulations with the three refrigerants, revealing the most notable tendencies of the electric and mechanical power (kW) in addition to the values of heat transferred through the two heat exchangers: evaporator and condenser.

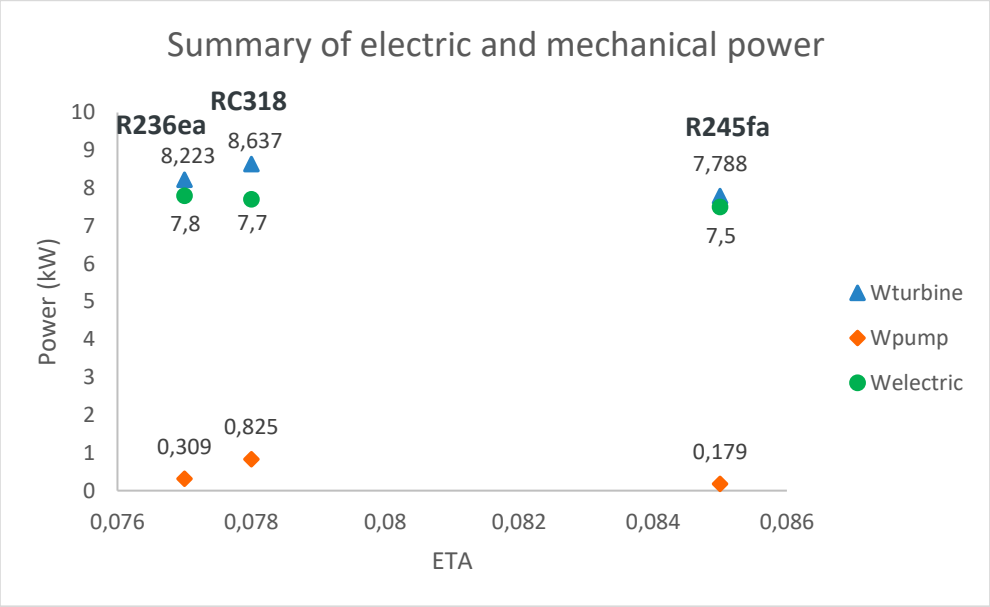

Figure 28. Summary of electric and mechanical power (kW) for the three working fluids.

One of the clearest conclusions deduced is that the highest power required for the pump operation arises from the RC318 cycle performance, so that the difference between the power obtained with the turbine and the final electric power is almost 1kW. Moreover, the highest mechanical power resulted from the turbine expansion does not turn out to be the highest final electric power nor the highest efficiency (ETA).

On the other hand, the lowest power needed in the pump results when the working fluid is R245fa, which is also the one that provides highest efficiency. However, although the refrigerant

R236ea results in a lower efficiency, the power required in the pump is likewise small and the final electrical power is the highest.

According to *Figure 29*, and as it has been previously explained, the higher the heat transferred through the evaporator is, the lower the efficiency reached is. This chart also reflects the same influence with the heat required for the fluid cooling in the condenser.

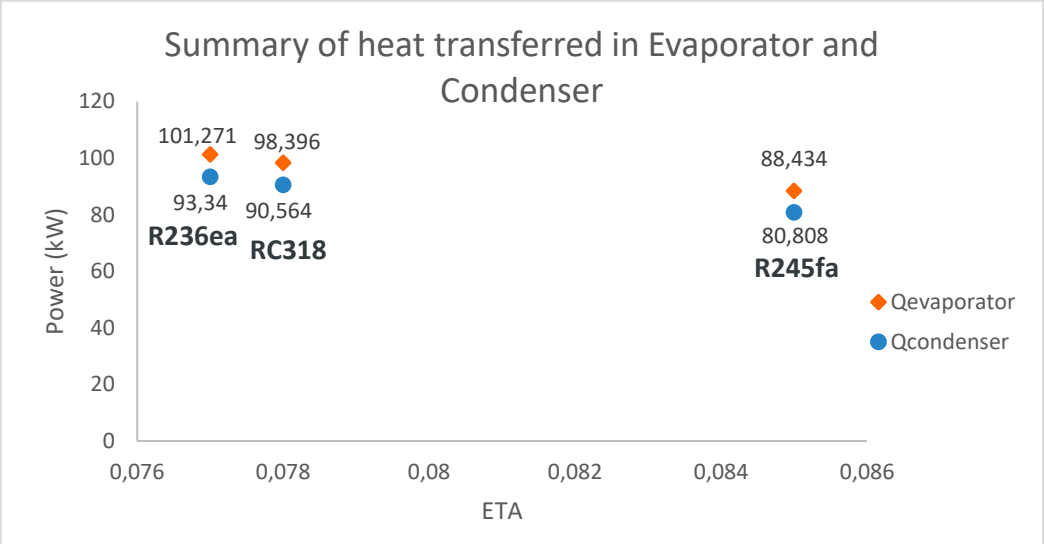

Figure 29. Summary of heat transferred in Evaporator and Condenser.

Finally, in order to have an easier overview of the three cycles temperature and pressure levels, as well as their specific net work, a graph gathering the three T-s diagrams was developed (see *Figure 30*). The main conclusions are the following:

- The evaporating and condensing temperatures are similar for the three fluids.
- The specific net work performed is higher for R245fa (bigger inner area of the cycle), however the final power is lower due to the smaller mass flow.
- The only outcome with overheating is the optimal cycle for R245fa (26 °C of superheating). The major disadvantage of being a dry fluid with overheating is that this implies a higher cooling load in the condenser.

Regarding the overheating issue and observing that the evaporating temperatures lie far from the 100 °C temperature of the heat source, it could be wondered why the best result for R245fa involves a high superheating whereas the best results for R236ea and RC318 do not. When a superheating is set for both working fluids, it involves a reduction in the performed net electric power when the efficiency is equal. This issue is explained with more detail in the following heading: *3.3.3. Effect of overheating in the system efficiency*.

For the reasons mentioned before, the fluid selected as optimum is R236ea:

- It results in the highest final electric power (7,8 kW instead of 7,5 or 7,7 kW).
- Even if the efficiency is the lowest, the three values are very similar.
- The power used from the waste heat in the evaporator is the highest

R236ea

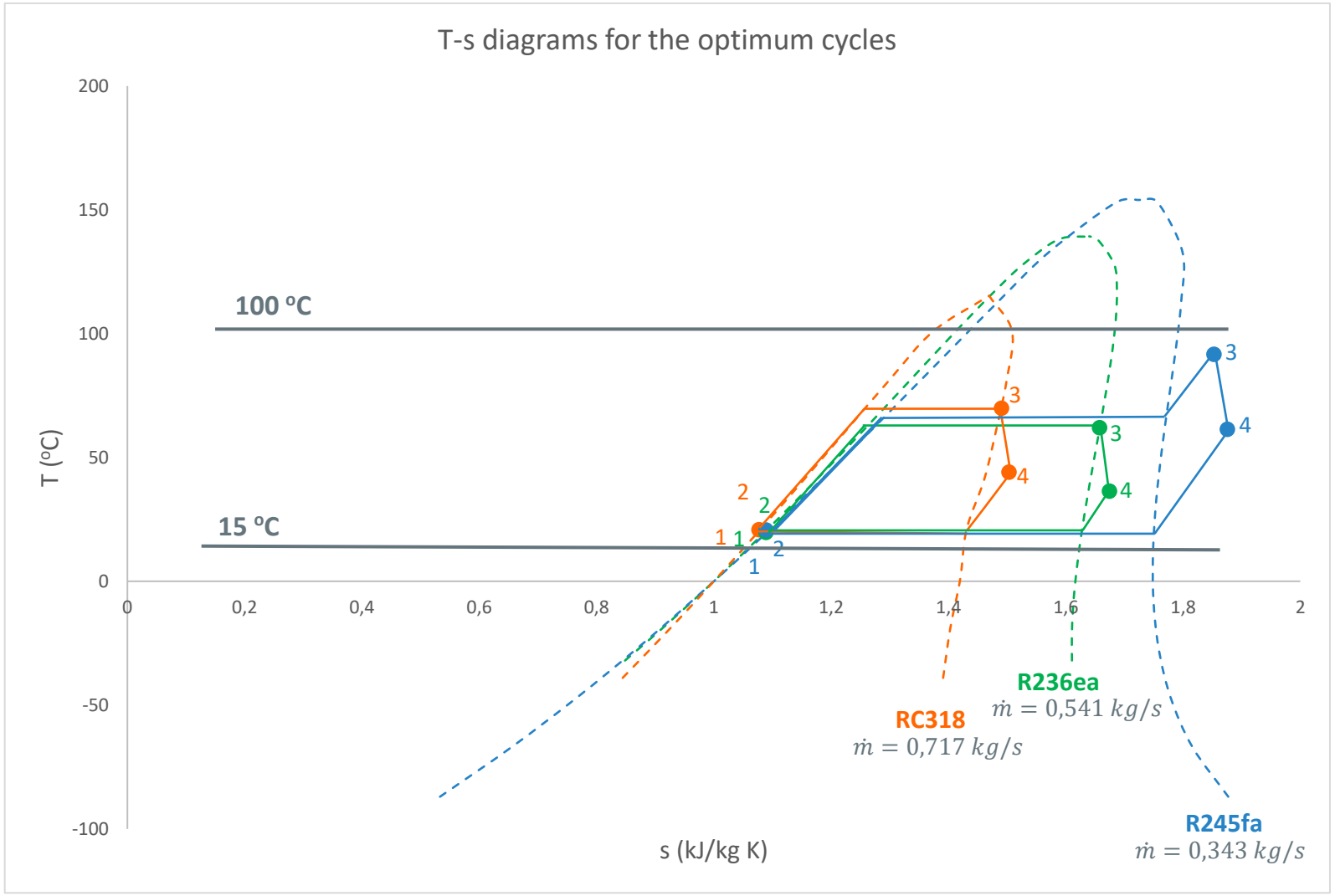

Figure 30. T-s diagrams with the optimum cycles for the fluids: RC318, R236ea and R245fa.

3.3.3. Effect of overheating in the system efficiency

As can be assessed from *Figure 27*, when the software Ebsilon iterates to find the optimal cycle, the point 3 is located on the saturated vapor line (limit of the two-phases mixture: steam and liquid). In order to make sure that there are no droplets at the entrance of the expander, with the possibility of damaging the turbine blades, a small overheating is considered necessary. For that reason, the cycle selected was modified adding a 5K superheating, which implies as well, the removal of the controller. As a result, the output of the evaporator is doubtlessly superheated vapor, avoiding the presence of unwished humidity.

Some authors, such as Bao et al. [1] or Liu et al. [18] already inquired that when the fluid is "dry" the overheating implies a reduction in the efficiency or electric power accomplished. Although this issue is true, as can be seen in *Figure 31*, the benefits of the overheating get over the depletion in electrical performance, which is not significant.

Figure 31 and *Figure 32* exhibit the results after the Ebsilon simulation, establishing the 5K overheating.

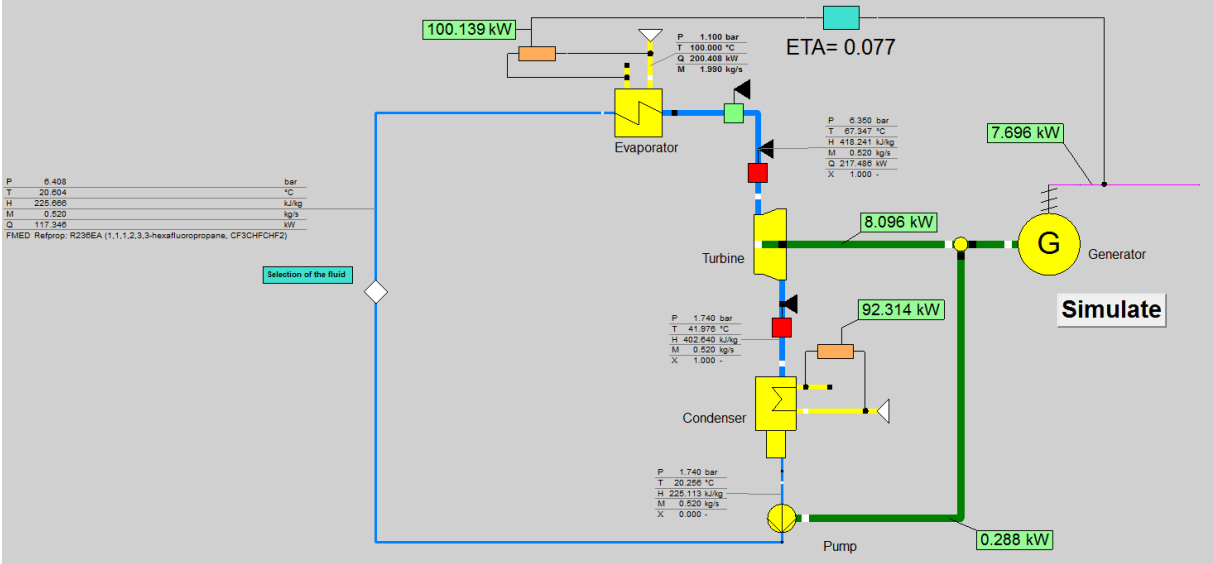

Figure 31. Model for R236ea with 5K overheating.

Point	Without overheating				With 5K overheating			
	T (ºC)	P (bar)	H (kJ/kg)	m (kg/s)	T (ºC)	P (bar)	H (kJ/kg)	m (kg/s)
1	20,256	1,740	225,113	0,5414	20,256	1,740	225,113	0,5200
2	20,619	6,413	225,684		20,604	6,408	225,666	
3	61,950	6,350	412,735		67,347	6,350	418,241	
4	36,280	1,740	357,516		41,976	1,740	402,640	

Table 16. Comparison of main parameters without and with 5K overheating for the fluid R236ea.

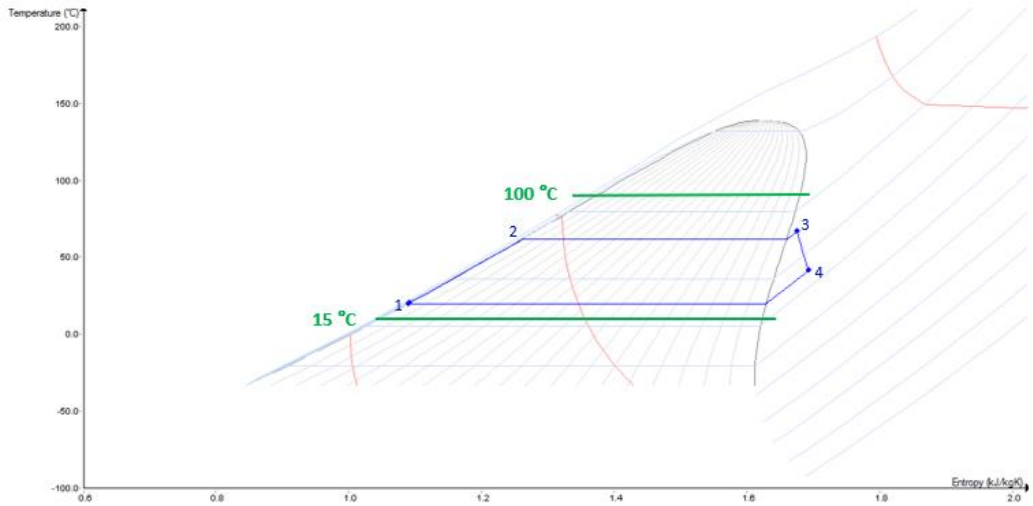

Figure 32. T-s diagram for R236ea with 5K overheating.

	Without overheating	With 5K overheating	Variation
$\dot{W}_{electric}$ (kW)	7,8	7,696	-0,104 (-1,3 %)
$\dot{W}_{turbine}$ (kW)	8,223	8,096	-0,127 (-1,5 %)
$\dot{W}_{pump}$ (kW)	0,309	0,288	-0,021 (-6,8 %)
$\dot{Q}_{evaporator}$ (kW)	101,271	100,139	-1,132 (-1,1 %)
$\dot{Q}_{condenser}$ (kW)	93,340	92,314	-1,026 (-1,1 %)
Efficiency (ETA)	0,077	0,077	0
References in the document	*Figure 26, Figure 27 Table 14, Table 15*	*Figure 31, Figure 32*	-

Table 17. Comparison of main results without and with 5K overheating for the fluid R236ea.

Regarding *Table 17* and *Table 16,* the succeeding statements can be noticed:

- The electric power is only reduced in 0,1 kW (1,3% lower than the original one) but the power required for the pump operation is decreased in a higher proportion (6,8%).
- The efficiency remains constant.
- It involves the advantage of avoiding the possibility of droplets that could damage the turbine blades.

In conclusion, the cycle described above is the one selected as the optimal one for the system operation.

3.3.4. Boundaries for the fluid R236ea

Through this work, the procedure of selecting the working fluid as well as the main parameters for the ORC turbomachine has been related to different kind of boundaries:

- Firstly, the market analysis defined the conditions for the input at the evaporator (200 kW of air at 100 °C), which is an important threshold for the cycle operating.
- Secondly, the physical properties and the environmental and safety concerns reduced the group of working fluids that should be screened during the simulations.

- To make the simulations more realistic, the isentropic efficiencies in both turbine and pump were established in a lower value than the default in Ebsilon, leading to another technical threshold.
- Finally, throughout the simulations, some other physical boundaries were achieved, depending on the parameters set. Those are the ones that are explained across this section.

a) Boundaries with the controller to fix the performed electric power

Bearing in mind what has been explained in the previous section, the simulations were carried out setting a net electric power in the controller, which modifies the mass flow of the working fluid in order to achieve the established power. To perform the simulations, a lower pressure level was determined for a condensing temperature around 20 ºC and the higher pressure level was decreased in each iteration, starting with the pressure corresponding to the evaporating temperature of 100 ºC.

Although the viable results for each of the working fluids studied are gathered in *Table 9*, through this section the R236ea cycle thermodynamic boundaries are analysed. For the rest of the working fluids the following discussions could be also applied due to their similar behaviour.

The two possible situations of error found are:

Situation 1 of error

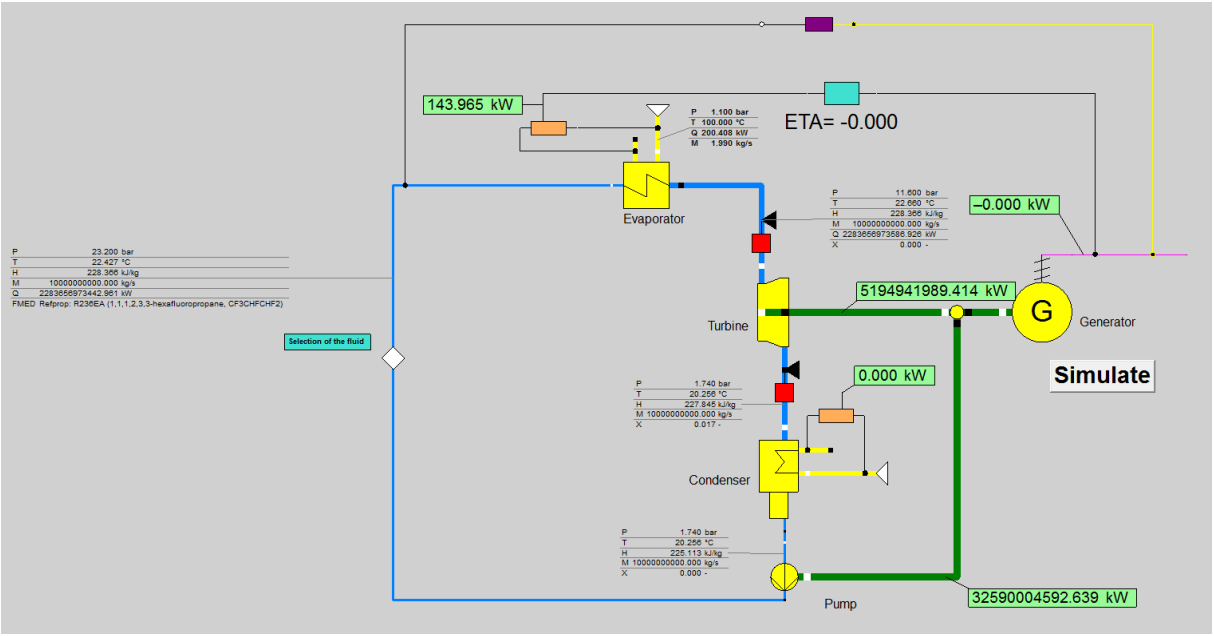

Figure 33. Situation 1 of error for the fluid R236ea.

- The work required for the pump operation is above the work obtained with the turbine expansion in a big quantity: W_{pump} >> $W_{turbine}$. Consequently, the electric outcome is below 0.
- Large pressure losses in the evaporator (above 10 bar). Therefore, the working fluid mass flow reaches the maximum value allowed in Ebsilon: higher than 10^{10} kg/s.

- Pinch point violation in the condenser, which involves a high air mass flow to make it feasible.

Situation 2 of error

- The input of the turbine has a degree of humidity, with a mix of vapor and liquid, resulting in a steam rate lower than one: $X_3 < 1$. This is related with the power supplied in the Evaporator (first threshold derived from the market analysis), which is not enough to upgrade the working fluid mass flow until the vapor saturation point.

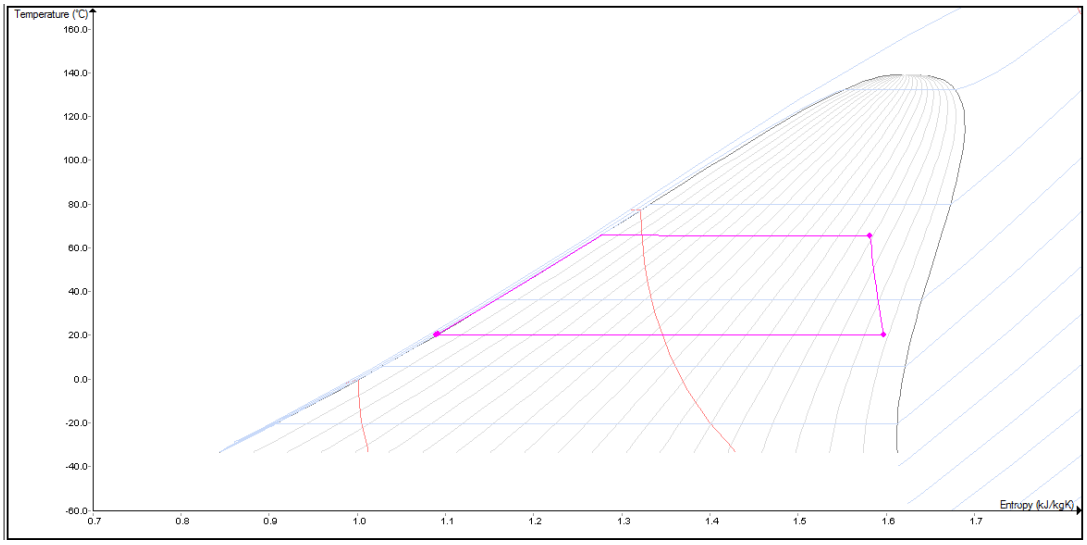

Figure 34. Situation 2 of error for the fluid R236ea.

Table 18 and *Table 19* show the results after the simulations for two different electric powers (8 and 7,8 kW) established as the target variable in the controller. The tables display the different ranges of pressure and temperature as evaporating level and the situation of error related to each of them.

8 kW		
Condensing level	**Evaporating level**	**Situation of error**
1,74 bar 20,25 °C	> 11,65 bar | > 86,42 °C	1
	11,65 – 4,95 bar | 86,42 – 52,9 °C	2
	< 4,95 bar | < 52,9 °C	1
1,84 bar 21,81 °C	> 10,85 bar | > 83,36 °C	1
	10,85 – 5,25 bar | 83,36 – 54,99 °C	2
	< 5,25 bar | < 54,99 °C	1
1,94 bar 23,3 °C	> 10,55 bar | > 82,17 °C	1
	10,55 – 5,75 bar | 82,17 – 58,27 °C	2
	< 5,75 bar | < 58,27 °C	1

Table 18. Thermodynamic borders of the fluid R236ea for 8 kW of net electric power.

7,8 kW		
Condensing level	**Evaporating level**	**Situation of error**
1,74 bar 20,25 ºC	> 11,45 bar | > 85,67 ºC	1
	11,45 – 6,35 bar | 85,67 – 61,94 ºC	2
	6,35 – 6,15 bar | 61,94 – 60,75 ºC	Feasible cycle
	6,15 – 5,75 bar | 60,75 – 58,27 ºC	2
	< 5,75 | < 58,27 ºC	1

Table 19. Thermodynamic borders of the fluid R236ea for 7,8 kW of net electric power.

When rising the condensing level in *Table 19*, similar results were obtained but performing a lower final electric power.

b) Boundaries without the controller and with a 5K superheating

After these tests, a different type of simulation was carried out. That analysis consisted on removing the controller and setting different pressure levels (both evaporating and condensing). The aim of this was verifying if the boundaries without establishing a predeterminate electric power (allowing the cycle to accomplish lower outcomes) were similar to the ones obtained when a controller was fitted to achieve a specific performance. When conducting these simulations, the main error found was:

Situation 3 of error

- Pinch point violated in evaporator.

Unlike what happens when there is a pinch point violation in the condenser, the conditions in the evaporator cannot be modified because they are the input data obtained from the market analysis and the criteria for which the system needs to be designed. That is to say, it is the first boundary determined and cannot be altered for this study.

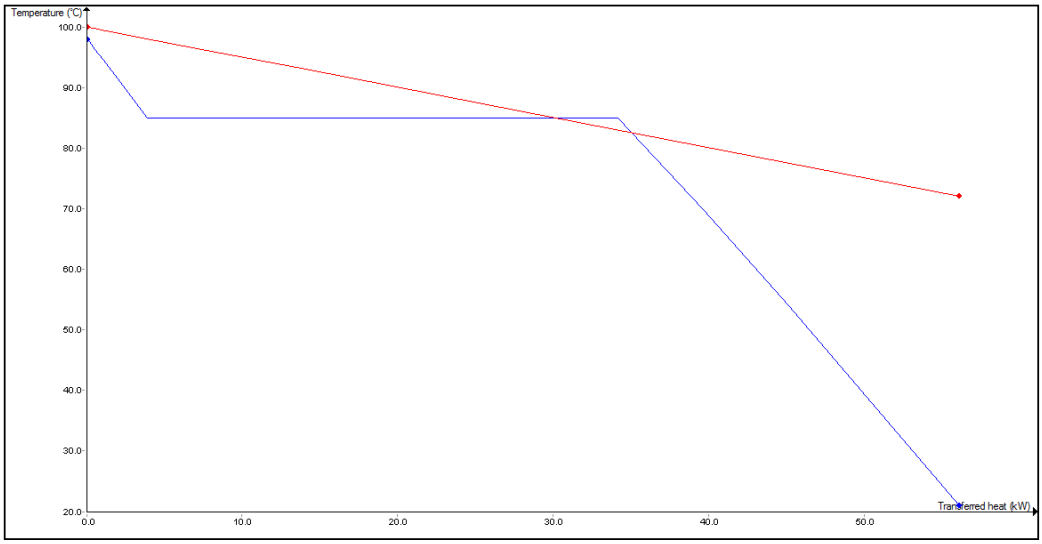

Figure 35. Situation 3 of error for the fluid R236ea.

Table 20, *Table 21* and *Table 22* feature the results when simulating under these conditions. These results show again that when increasing the condensing pressure, the cycle outcome is lower.

Condensing level	Evaporating level	Situation of error
1,74 bar 20,25 ºC	> 6,35 bar | > 61,94 ºC	3
	< 6,35 bar | < 61,94 ºC	Feasible cycle $\dot{W}_{electric} = 7{,}696\ kW$

Table 20. Thermodynamic borders for 1,74 bar of condensing pressure without controller and with 5K superheating.

Condensing level	Evaporating level	Situation of error
1,84 bar 21,81 ºC	> 8,27 bar | > 72,15 ºC	3
	< 8,27 bar | < 72,15 ºC	Feasible cycle: $\dot{W}_{electric} = 6{,}783\ kW$

Table 21. Thermodynamic borders for 1,84 bar of condensing pressure without controller and with 5K superheating.

Condensing level	Evaporating level	Situation of error
1,94 bar 23,30 ºC	> 7,27 bar | > 67,09 ºC	3
	< 7,27 bar| < 67,09 ºC	Feasible cycle: $\dot{W}_{electric} = 6{,}928\ kW$

Table 22. Thermodynamic borders for 1,94 bar of condensing pressure without controller and with 5K superheating.

4. Equipment required for the ORC integrated system

4.1. Heat exchangers for the Evaporator and Condenser

The ORC integrated system needs two heat exchangers: one to work as evaporator and the other to operate as condenser. When the simulations in Ebsilon were carried out, the parameter *K·A* (kW/K) was displayed with the values showed in *Table 23*. *K* refers to the global heat transmission coefficient and *A* to the heat transmission surface.

Considering that the global heat conductivity (*K*) could be estimated as the highest among all (working fluid, wall of the heat exchanger and air), an assessment of the heat exchanger area could be performed. This is useful to have a rough estimate of the size that both devices would have. The value taken for *K* is 1200 W/m^{2}K, regarding that the highest heat conductivity among the three media would be the one of the working fluids and that 1200 could be an appropriate average value for testing:

$$K \cdot A \approx 1200 \, \frac{W}{m^2 \, K} \cdot A$$

	Evaporator	Condenser
K·A (kW/K)	4,7813	6,0067
A (m^2)	3,98	5

Table 23. Parameters K·A of the heat exchangers in Ebsilon and estimated areas.

4.2. Main parameters of the turbine and pump engines

With the aim of studying which are the viable options in the engines design for the cycle selected as optimal, a study based on the Cordier diagram was carried out. In 1953, Otto Cordier linked the optimum operating conditions (i.e. the volumetric flowrate $\dot{V}_{opt}$ and the specific head $Y = \Delta p_{opt}/\rho$), with the optimum diameter D and speed n, for one-stage machines operating at optimum efficiency. This was performed with the support of speed and diameter numbers which are defined as:

$$\sigma = 2\sqrt{\pi}\, n \, \frac{\sqrt{\dot{V}}}{(2Y)^{3/2}}$$

Equation 9. Speed number.

$$\delta = \frac{\sqrt{\pi}}{2} \, D \, \sqrt[4]{\frac{2Y}{\dot{V}^2}}$$

Equation 10. Diameter number.

Cordier plotted the optimum values σ_{opt} and δ_{opt} on a logarithmic graph, as shown, in the original representation of Cordier in *Figure 36*. In this way, for all classical impeller types it could

be obtained a reasonably well-defined curve known as the Cordier curve. Through experiments carried out for different types of fans, blowers, and pumps, Cordier could show that axial turbomachines possess high speed σ and low diameter δ numbers, whereas radial turbomachines are characterized by low speed numbers and high diameter numbers. Diagonal machines are in the range of medium values of speed numbers σ and diameter numbers δ. Although this diagram does not show details of the blade shape in the design of turbomachines, it is definitely useful to make basic decisions on the type of machine to be selected for the particular operating point (i.e. for the head and flowrate to be achieved) [35].

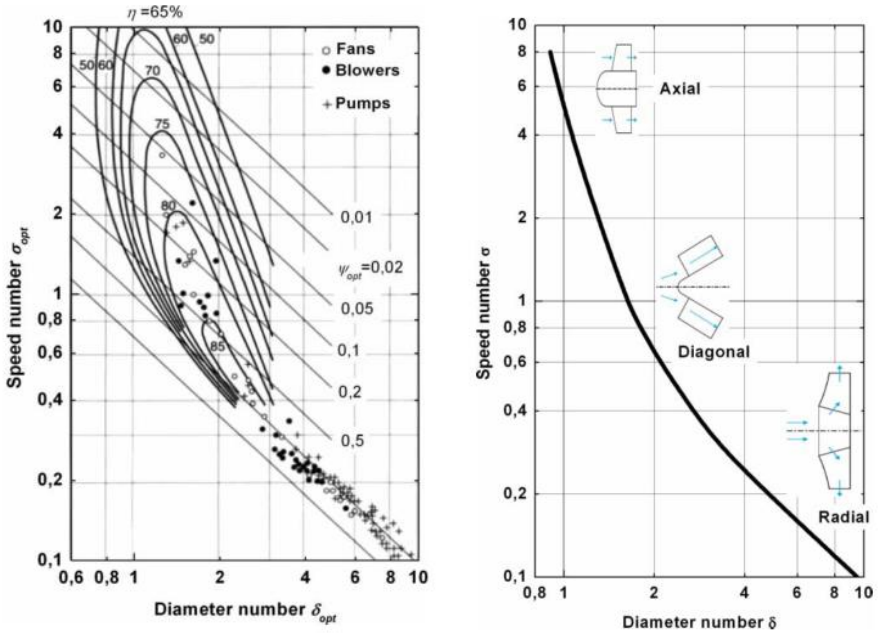

Figure 36. Original performance diagram of turbomachines introduced by Cordier in 1953 [35].

Due to the engines, pump and turbine, considered within this work are planned to be one-stage, it is appropriate using the Cordier diagram as a tool to define the fundamental parameters. The most important criteria characterizing the engines are the diameter of the plates (considering an average value) and the number of rotations.

The power obtained from the turbine (equation in the left) and the pump (equation in the right), are determined with the following expressions, where Δh_s defines the isentropic enthalpic difference between the device inlet and outlet, and $\eta_{turbine}$ or η_{pump} represent the isentropic efficiencies for the turbine and the pump respectively (previously established in *Table 7*).

$$\dot{W}_{turbine} = \dot{m}\,\Delta h = \dot{m}\,\Delta h_s\,\eta_{turbine} \qquad \dot{W}_{pump} = \dot{m}\,\Delta h = {}^{\dot{m}\,\Delta h_s}/_{\eta_{pump}}$$

$$u = \pi\,D\,n$$

Equation 11. Circumferential speed.

$$C_m = \frac{\dot{V}}{A} = \frac{\dot{m}\,v}{\pi\,D\,B}$$

Equation 12. Meridian velocity.

After defining the parameters u (circumferential velocity) and C_m (meridian velocity), the flow and head numbers, in which the Otto Cordier diagram are based on, can be determined. Calculating these coefficients leads to an easier procedure with respect to the engines criteria selection.

$$\varphi = \frac{C_m}{u} = \frac{\dot{m}\, v}{\pi\, D\, B} \frac{1}{\pi\, D\, n}$$

Equation 13. Flow number.

$$\psi = \frac{\Delta h_{s,1\ stage}}{u^2/2} = 2\frac{\Delta h_{s,1\ stage}}{(\pi\, D\, n)^2}$$

Equation 14. Head number.

4.2.1. Main parameters of the turbine engine

In *Figure 37* the main parameters of a one-stage radial turbine are represented:

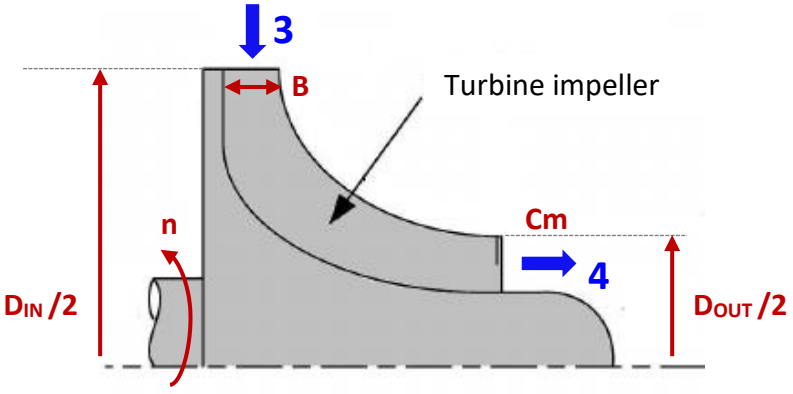

Figure 37. Parameters in the radial turbine.

In order to calculate the necessary framework to use the Cordier diagram, *Table 24* collects the stream values at the inlet and outlet of the turbine (data taken from *Table 16*), so that it is possible to determine the optimal diameters and rotation speed for the specific cycle selected as most suitable to recovery the waste heat source:

Inlet turbine		Outlet turbine	
P_3 (bar)	6,35	**P_4 (bar)**	1,74
h_3 (kJ/kg)	418,24	**h_4 (kJ/kg)**	402,64
$\eta_{turbine}$	0,75	**$\eta_{turbine}$**	0,75
v_3 (m^3/kg)	0,02500	**v_4 (m^3/kg)**	0,09422
m (kg/s)	0,52	**m (kg/s)**	0,52

Table 24. Results at the inlet and outlet of the turbine.

Taking into account the data in *Table 24*:

$$\Delta h_{s,1\ stage} = \frac{h_3 - h_4}{\eta_{turbine}} = \frac{418{,}24 - 402{,}64}{0{,}75} = 20{,}8\ kJ/kg$$

Addressing the Cordier diagram, *Figure 38* shows the different combinations of ψ (flow number) and φ (head number) possible for a radial turbine. The main reason why only radial alternatives where accounted is that it ensures a more compact and cheaper final design.

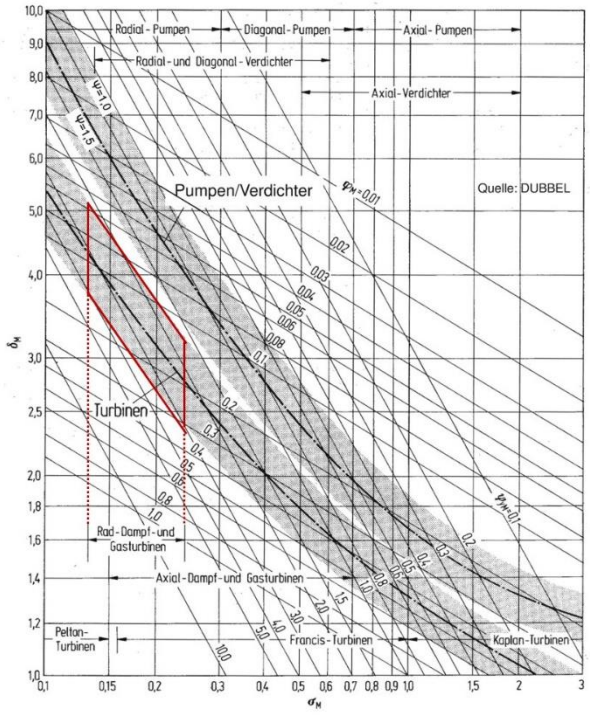

Figure 38. Range of ψ and ϕ for a radial turbine in Cordier diagram.

Considering the points within the area surrounded by the red line (first two columns in *Table 25*) the diameters at the inlet and outlet of the turbine as well as the number of rotations and the average speed for the working fluid at the output of the device were calculated. It is important to highlight that the pairs which result in higher outlet diameter than inlet diameter of the device are not valid, as can be observed in *Figure 37*.

B = 3,5 mm						
Ψ	**φ**	**D_{IN} (mm)**	**D_{OUT} (mm)**	**n (1/min)**	**Cm (m/s)**	**$D_{OUT} < D_{IN}$?**
3	0,1	100	73	22395	11,776	yes
3	0,2	50	51	44791	23,551	no
2	0,08	102	74	26874	11,538	yes
2	0,1	82	66	33593	14,422	yes
2	0,2	41	47	67186	28,844	no

Table 25. Parameters for turbine from Cordier diagram with B = 3,5 mm.

Different values for the width of the turbine blade (parameter B) were tested in order to compare the feasible results reached. *Table 25* is the example of one of them, while the rest are displayed in the annex (*A1. Main parameters of the turbine engine*). To understand easier the viable combinations of diameters (inlet and outlet) and rotation speed derived from the variation of the width (B), *Figure 39* displays the alternatives.

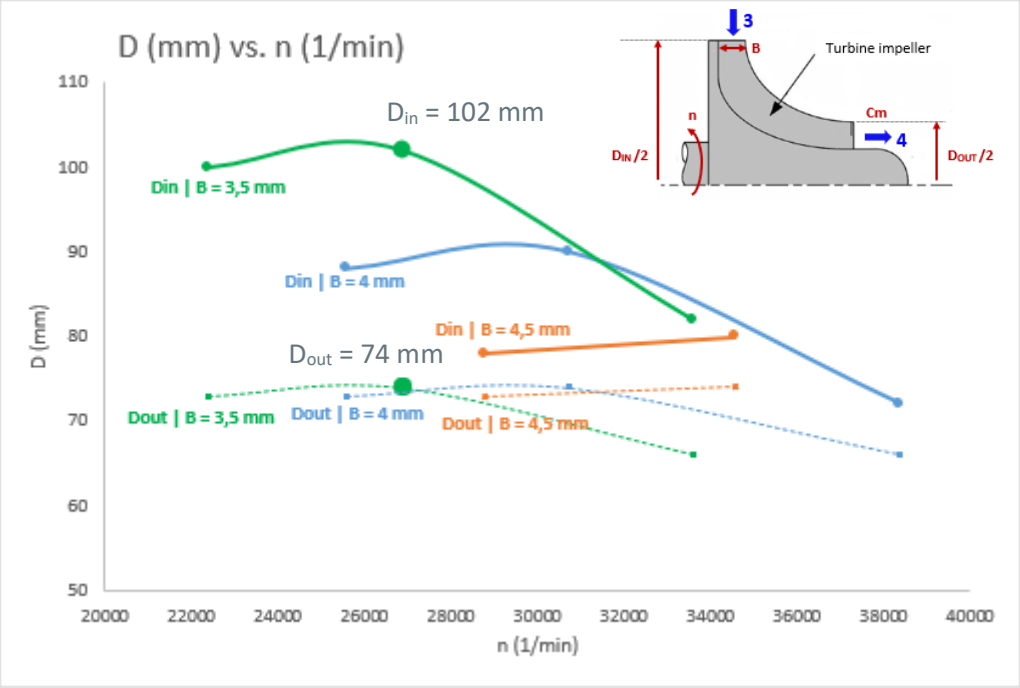

Figure 39. Combination of D (mm) and n (1/min) possible for the radial turbine.

With the purpose of assessing the first primary design, it is essential to understand that the higher the difference between the inlet and outlet diameters is, the higher the engine performance tends to be. Considering this, it is possible to determine the optimal main dimensions and rotation speed of the turbine. On the basis of the results, the point which provides a higher difference between both diameters has been highlighted in both *Table 25* and *Figure 39*, and reflected in *Table 26*:

n (1/min)	26874
D_{IN} (mm)	102
D_{OUT} (mm)	74
B (mm)	3,5

Table 26. Optimal dimensions and rotation speed for the turbine engine.

It is crucial to emphasize that even if these seem to be the best results obtained from this preliminary design, boundary layer effects were not considered. Therefore, after a more intensive analysis and detailed design, it is possible that the optimal dimensions and rotation speed result from a wider blade width, reaching a state of commitment between both issues.

4.2.2. Main parameters in the pump engine

Similar to the procedure followed for the turbine, the pump included in the ORC system is a radial and single-stage device. The main parameters that should be considered in the first steps of the pump design are the ones described in *Figure 40*.

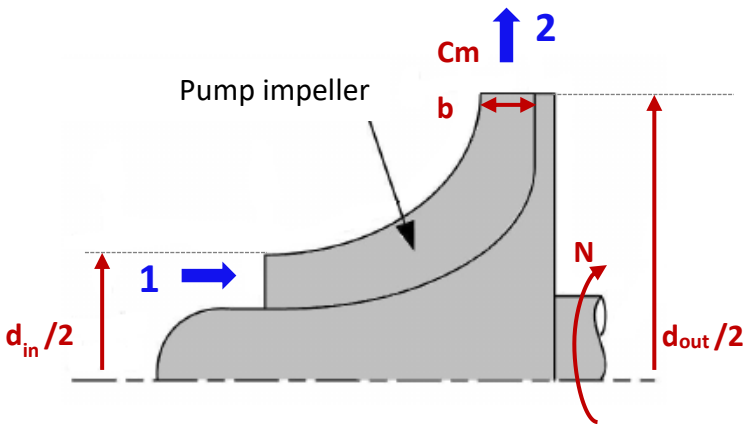

Figure 40. Parameters in the radial pump.

Table 27 contains the input and output data of the pump that were obtained from the cycle performance in Ebsilon (data taken from *Table 16).*

Inlet turbine		Outlet turbine	
P_1 (bar)	1,74	**P_2 (bar)**	6,4
h_1 (kJ/kg)	225,11	**h_2 (kJ/kg)**	225,66
η_{pump}	0,6	**η_{pump}**	0,6
v_1 (m^3/kg)	0,00069	**v_2 (m^3/kg)**	0,00069
m (kg/s)	0,52	**m (kg/s)**	0,52

Table 27. Results at the inlet and outlet of the pump.

Taking into account this information:

$$\Delta h_{s,1\ stage} = (h_2 - h_1)\,\eta_{pump} = (225{,}66 - 225{,}11)\,0{,}6 = 0{,}33\ kJ/kg$$

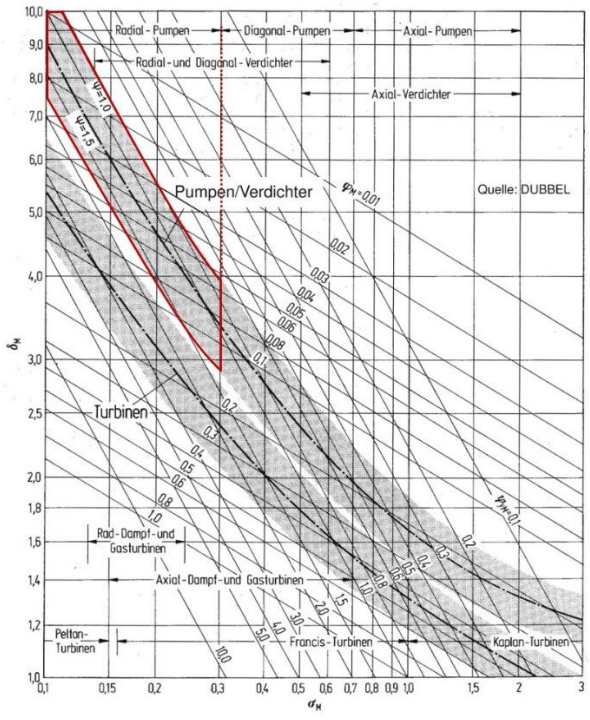

Figure 41. Range of ψ and ϕ for a radial pump in Cordier diagram.

Considering the possible combinations of the head and flow numbers, and varying the width of the impeller blade, the inlet and outlet diameters were calculated, as well as the rotation speed of the engine. One example of this calculations for b = 3,5 mm is gathered in *Table 28*. In this case, it is essential to verify that the outlet diameter is bigger than the inlet, in order to make the result feasible.

b = 3,5 mm						
Ψ	**φ**	**d_{in} (mm)**	**d_{out} (mm)**	**N (1/min)**	**Cm (m/s)**	**$d_{out} > d_{in}$?**
1,5	0,1	15	16	27072	2,098	yes
1,5	0,08	17	20	24214	1,678	yes
1,5	0,06	19	26	20970	1,259	yes
1,5	0,05	21	31	19143	1,049	yes
1,5	0,04	23	39	17122	0,839	yes
1,5	0,03	27	52	14828	0,629	yes
1,5	0,02	33	78	12107	0,42	yes
1	0,08	15	16	32820	2,055	yes
1	0,06	17	21	28423	1,541	yes
1	0,05	19	26	25947	1,285	yes
1	0,04	21	32	23207	1,028	yes
1	0,03	24	43	20098	0,771	yes
1	0,02	30	64	16410	0,514	yes
0,8	0,06	16	19	33601	1,723	yes
0,8	0,05	18	23	30673	1,436	yes
0,8	0,04	20	29	27435	1,149	yes
0,8	0,03	23	38	23760	0,862	yes
0,8	0,02	28	57	19400	0,574	yes
0,8	0,01	40	114	13718	0,287	yes

Table 28. Parameters for the pump from Cordier diagram with b = 3,5 mm.

Evaluating the outcomes obtained after the whole calculation process (see *A2. Main parameters of the pump engine*), the one that offers the highest difference between the inlet and outlet diameter is the one emphasized in *Table 28* and *Figure 42*. This graph features the possible combinations of diameters and rotation speed for a one-stage radial pump, with an impeller width of 3,5 mm, operating in the conditions determined by *Table 27*.

The rest of the charts regarding the different widths tested are as well collected in the annex *A2. Main parameters of the pump engine*, where it is possible to see that the optimal dimensions seem to be the ones described above and highlighted in *Table 29*. Similar to what was discussed for the turbine, the width of the blade is in the limit of the efficient feasibility, in term of effects like the boundary layer. For this reason and considering this is only a prior design, it is necessary to carry out a more comprehensive study.

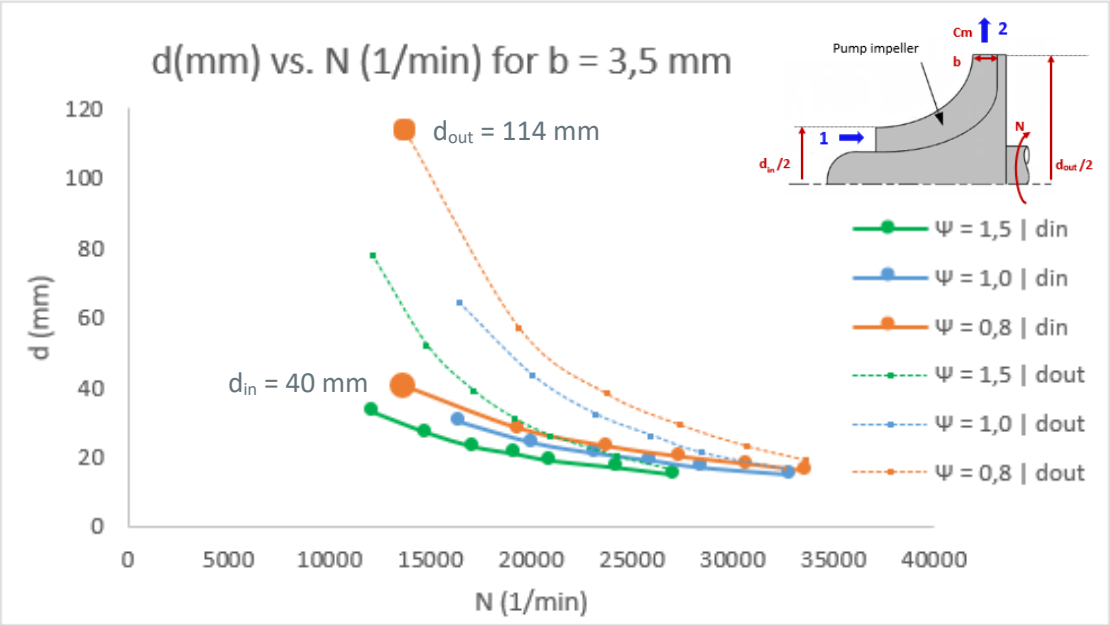

Figure 42. Combination of d (mm) and N (1/min) possible when b = 3,5 mm for the radial pump.

N (1/min)	13718
d_{in} (mm)	40
d_{OUT} (mm)	114
b (mm)	3,5

Table 29. Optimal dimensions and rotation speed for the pump engine.

In the model designed for the system in Ebsilon (see *Figure 2*) the power required in the pump shaft is provided by the mechanical output obtained after the turbine expansion. Accounting the optimal rotation speeds discussed in *Table 26* and *Table 29* for both engines, it can be noticed that the rotation speeds result in different values: nearly 26.900 min^{-1} for the turbine while closed to 13.700 min^{-1} for the pump. Hence, the implementation of a novel planetary transmission is necessary, so that both engines can be implemented in the same integrated system but rotating at their optimal speeds (which are different), as shown in *Figure 43*. The gear that rotates faster (the internal one) is connected to the turbine due to its higher rotation velocity, while the three externals should be linked to the pump shaft due to its lower rotation speed.

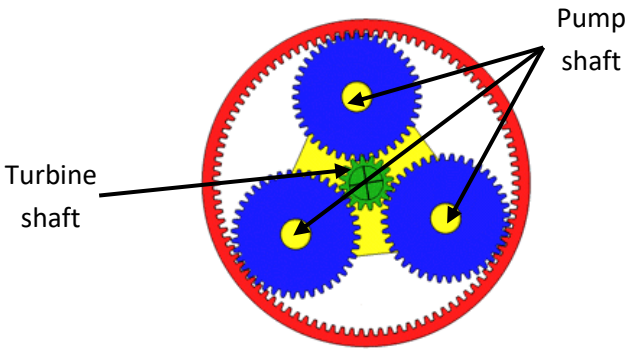

Figure 43. Planetary transmission.

5. Conclusions and next steps

5.1. Conclusions

In recent years, the use of low-grade waste heat from industrial areas has received increasing attentions. This is not only for its potential in reducing fossil fuel consumption and alleviating environmental concerns, but also because of its potential to optimize companies' resources and profit in producing electricity from the heat currently wasted due to their regular processes. Since conventional steam power cycles cannot give a better performance to recover low-grade waste heat (the largest amount of residual heat released to the environment), the organic Rankine cycle (ORC) is proposed to recover these low temperature sources into electricity, mainly in the temperature range from 100 to 400 ^{o}C.

However, depending on the conditions of the heat source, which are broadly diverse, the optimal criteria for the ORC system development are different. For that reason, through the present work it was analysed the waste heat offer in Europe so that the ORC cycle was designed on the basis of the middle of the market deduced. That is to say, regarding the most frequent criteria of the heat sources currently released to the environment, so that the ORC discussed is designed to recover these potential sources.

5.1.1. Conclusions regarding the waste heat market analysis

Thus, the first step carried out was the market analysis on the waste heat in Europe. The main conclusions regarding this task are the following:

- The largest amounts of waste heat available are highly concentrated in the low-temperature levels. However, there are not still enough efficient technologies developed to recover these sources.
- Nowadays, increasing attention is being paid in reducing the environmental concerns and fossil fuel consumptions. For this reason, not only independent researchers are focusing on finding efficient solutions to take advantage of the potential waste heat, but also many funds within the European framework are currently intended to find improvements on these topics.
- Even if great efforts are being made in this field, there are not many resources that collect data from the industries residual heat. In some cases, this information is a rough estimation (i.e. Spanish meat map) and without specific data about temperature level or heat carrier.
- The regions of Saxony and Bavaria in Germany have their own heat maps. These maps, specially the Bavarian one, contain broader information about the residual heat offered by the companies.

- After the market analysis was performed with the data contained in Bavaria map at temperatures between 100 and 400 ^{o}C, the middle of the market (200 kW of air at 100 ^{o}C) was selected providing the input heat source for the ORC in the following steps of the study.

5.1.2. Conclusions regarding the ORC fluid and parameters selection

After the middle of the market was established, the next objective to perform was determining the optimal conditions for the ORC system operation.

- The selection of the proper fluid is one of the most important tasks when assessing the ORC working conditions. Although the alternative working fluids for an ORC could be almost countless, there are several boundaries that should be taken into account.
- The first inference was to select a “dry” pure fluid so that an unwished presence of droplets that could damage the turbine blades is avoided.
- According to the physical as well as environmental and safety concerns, the group of fluids to be screened in the follow-up simulations in Ebsilon software was reduced until: R236ea, R227ea, RC318 and R245fa.
- In order to select the optimal fluid and conditions for a high system performance, various simulations were carried out in Ebsilon. The results showed that, among the four possible working fluids, the one that resulted in highest net electric power was R236ea. That is the main reason why this fluid and its best performance (adding a 5K overheating) were selected as optimal for the heat source recovery.
- Then, two different types of simulations were developed (with a controller trying to reach a set electric power, and without controller) in order to determine the main boundaries of the system.

5.1.3. Conclusions about the ORC system equipment

When the optimal ORC requirements were established, a preliminary design of the system equipment was executed.

- The system entails two heat exchangers, working as evaporator and condenser. Ebsilon determines a value for their heat transfer coefficient multiplied by the area. This value allows to have an estimation of the transmission surface and consequently and idea of the size required for both devices.
- The preliminary design of the turbine and pump engines, studied as one-stage radial, was carried out on the basis of Cordier diagram. The main dimensions (inlet and outlet diameters) as well as the prior optimal rotation speed for each of them were determined.

- The results showed that the initial optimal rotation speeds were different for both engines (nearly 27.000 min^{-1} for the turbine and closed to 14.000 min^{-1} for the pump). This leads to the need of a novel transmission mechanism that allows the connection of both turbine and pump but rotating at different velocities.

5.2. Future steps

The future steps that should be conducted after this work are:

- Through this work only a preliminary study about the main dimensions for the turbine and pump engines has been carried out. This analysis was performed to establish the first system equipment criteria, verifying that the ORC thermodynamically viable leads to feasible machinery. Considering this, the principal future step to enforce is developing the detailed engineering.
- The concluded preliminary optimal rotation speeds displayed different values for both turbine and pump. In order to make the combined integrated machinery model achievable and at the same time allowing each of the engines to operate at their optimal velocities, it is required to develop an adequate and novel transmission, including planetary gears.
- To complete the components design, it is likewise necessary to find the most suitable heat exchangers to work as Evaporator and Condenser. This should take into account that the aim of this integrated turbomachine is to be as cheap and compact as possible.

Bibliography

[1] Bao J. and Zhao L. “A review of working fluids and expander selections for organic Rankine cycle”. *Renewable and Sustainable Energy Reviews,* vol. 24, pp. 325-342, 2013.

[2] Imran M. et al. “Recent research trends in organic Rankine cycle technology: A bibliometric approach”. *Renewable and Sustainable Energy Reviews,* vol. 81, pp. 552-562, 2018.

[3] Lion S. et al. “A review of waste heat recovery and Organic Rankine Cycles (ORC) in on-off highway vehicle heavy duty diesel engine applications”. *Renewable and Sustainable Energy Reviews,* vol. 79, pp. 691-708, 2017.

[4] Sprouse C. and Depcik C. “Review of organic Rankine cycles for internal combustion engine exhaust waste heat recovery”. *Appl Therm Eng,* vol. 51, 2013.

[5] Saidur R. et al. “Technologies to recover exhaust heat from internal combustion engines”. *Renewable and Sustainable Energy Reviews,* vol. 16, 2012.

[6] Tocci L. et al. “Small scale Organic Rankine Cycle (ORC): A techno-economic review”. *Energies,* vol. 10, p. 413, 2017.

[7] Rahbar K. et al. “Review of organic Rankine cycle for small-scale applications”. *Energy Convers Manag,* vol. 134, 2017.

[8] Chen H.; Goswami D.; Stefanakos E. “A review of thermodynamic cycles and working fluids for the conversion of low-grade heat”. *Renewable and Sustainable Energy Reviews,* vol. 14, no. 9, pp. 3059-3067, 2010.

[9] Modi A. and Haglind F. “A review of recent research on the use of zeotropic mixtures in power generation systems”. *Energy Convers Manag,* vol. 138, pp. 603-626, 2017.

[10] Bamorovat Abadi G. and Kim K. “Investigation of organic Rankine cyles with zeotropic mixtures as a working fluid: Advantages and issues”. *Renewable and Sustainable Energy Reviews,* vol. 73, 2017.

[11] Dai Y. et al. “Research progress of the Organic Rankine Cycle working fluids thermal stability". *Journal Eng Thermophys,* vol. 37, 2016.

[12] Imran M. et al. “Volumetric expanders for low grade & waste heat recovery applications”. *Renewable and Sustainable Energy Reviews,* vol. 57, pp. 1090-1109, 2016.

[13] Song P. et al. “A review of scroll expanders for organic Rankine cycle systems”. *Appl Therm Eng,* vol. 75, 2015.

[14] Lecompte S. et al. “Review of organic Rankine cycle (ORC) architectures for waste heat recovery”. *Renewable and Sustainable Energy Reviews,* vol. 47, 2015.

[15] Zhai H. et al. “Categorization and analysis of heat sources for organic Rankine cycles systems”. *Renewable and Sustainable Energy Reviews,* vol. 64, pp. 790-805, 2016.

[16] Drescher U. and Brugemann B. “Fluid selection for the Organic Rankine Cycle (ORC) in biomass power and heat plants”. *Appl Therm Eng,* vol. 27, 2007.

[17] Chen Y. et al. “A comparative study of the carbon dioxide transcritical power cycle compared with an Organic Rankine Cycle with R123 as working fluid in waste heat recovery” *Appl Therm Eng,* vol. 26, 2006.

[18] Liu BT.; Chien K.; Wang C. “Effect of working fluids on Organic Rankine Cycle for waste heat recovery”. *Energy,* vol. 29, 2004.

[19] Hung T. “Waste heat recovery of organic Rankine cycle using dry fluids”. *Energy Conversion and Management,* vol. 42, no. 5, pp. 539-553, 2001.

[20] "LOVE". *European Comission: CORDIS*, 2018. [Online]. Available: https://cordis.europa.eu/result/rcn/91332_es.html.

[21] "Un grupo de investigadores recupera calor residual de bajo grado". *European Comission: CORDIS.* 2018. [Online]. Available: https://cordis.europa.eu/news/rcn/122200_es.html.

[22] "Un motor alatamente eficiente que transforma agua caliente en electricidad". *European Comission: CORDIS, Horizon 2020*. 2018. [Online]. Available: https://cordis.europa.eu/result/rcn/205499_es.html.

[23] Dai Y. and Wang L. “Parametric optimization and comparative study of Organic Rankine Cycle (ORC) for low grade waste heat recovery”. *Energy Conversation and Management,* vol. 50, no. 3, pp. 576-582, 2009.

[24] Panayiotou G. et al. “Preliminary assessment of waste heat potential in major European industries”. *Energy Procedia,* vol. 123, pp. 335-345, 2017.

[25] Blesl M. et al. “Wärmeatlas Baden-Württemberg: Erstellung eines Leitfadens und Umsetzung für Modellregionen”. *Forschungsbericht. FZKA-BWPLUS,* 2005.

[26] Lutsch W. “Perspektiven der Fernwärme un der Kraft-Wärme-Kopplung-Ergebnisse und Schlussfolgerungen aus der AGFW-Studie Pluralistische Wärmeversorgung" *AGFW,* 2005.

[27] Brückner S. et al. “Industrial waste heat recovery technologies: An economic analysis of heat transformation technologies”. Applied Energy, vol. 151, pp. 151-167, 2015.

[28] “Mapa de calor residual de España”. *IDAE*. 2018. [Online]. Available: http://www.mapadecalor.idae.es/.

[29] “Energieportal Sachsen”. 2018. [Online]. Available: http://www.energieportal-sachsen.de/.

[30] “Energieportal Bayern”. 2018. [Online]. Available: http://geoportal.bayern.de/energieatlas-karten/?wicket-crypt=h4NlGvzw9m4&wicket-crypt=vHzEgYEaT2.

[31] Yu H.; Feng X.; Wang Y. “A new pinch based method for simultaneous selection of working fluid and operating conditions in an ORC (Organic Rankine Cycle) recovering waste heat”. *Energy,* vol. 90, pp. 36-46, 2015.

[32] Calm J. and Hourahan G. “Physical, Safety, and Environmental Data for Current and Alternative Refrigerants”. *23rd International Congress of Refrigeration,* p. 22, 2011.

[33] United States Environmental Protection Agency (EPA). 2018. [Online]. Available: https://www.epa.gov/snap/refrigerant-safety.

[34] Raleigh E. and March N. "New Refrigerants Designation and Safety Classifications". 2017. [Online]. Available: https://climate.emerson.com/documents/raleigh-%E2%80%93-new-refrigerants-designation-safety-classifications-en-us-3722162.pdf.

[35] Epple P.; Durst F.; Delgado A. “A theoretical derivation of the Cordier diagram for turbomachines”. *Proceedings of the Institution of Mechanical Engineers, Part C: Journal of Mechanical Engineering Science,* vol. 225, no. 2, pp. 354-368, 2011.

Annex

A1. Main parameters of the turbine engine

B = 4 mm						
Ψ	**φ**	**D_{IN} (mm)**	**D_{OUT} (mm)**	**n (1/min)**	**Cm (m/s)**	**$D_{OUT} < D_{IN}$?**
3	0,1	88	73	25595	11,776	yes
3	0,2	44	51	51189	23,551	no
2	0,08	90	74	30714	11,538	yes
2	0,1	72	66	38392	14,422	yes
2	0,2	36	47	76784	28,844	no

Table 30. Parameters for turbine from Cordier diagram with B = 4 mm.

B = 4,5 mm						
Ψ	**φ**	**D_{IN} (mm)**	**D_{OUT} (mm)**	**n (1/min)**	**Cm (m/s)**	**$D_{OUT} < D_{IN}$?**
3	0,1	78	73	28794	11,776	yes
3	0,2	39	51	57588	23,551	no
2	0,08	80	74	34553	11,538	yes
2	0,1	64	66	43191	14,422	no
2	0,2	32	47	86382	28,844	no

Table 31. Parameters for turbine from Cordier diagram with B = 4,5 mm.

B = 5 mm						
Ψ	**φ**	**D_{IN} (mm)**	**D_{OUT} (mm)**	**n (1/min)**	**Cm (m/s)**	**$D_{OUT} < D_{IN}$?**
3	0,1	70	73	31993	11,776	no
3	0,2	35	51	63987	23,551	no
2	0,08	72	74	38392	11,538	no
2	0,1	57	66	47990	14,422	no
2	0,2	29	47	95980	28,844	no

Table 32. Parameters for turbine from Cordier diagram with B = 5 mm.

B = 5,5 mm						
Ψ	**φ**	**D_{IN} (mm)**	**D_{OUT} (mm)**	**n (1/min)**	**Cm (m/s)**	**$D_{OUT} < D_{IN}$?**
3	0,1	64	73	35193	11,776	no
3	0,2	32	51	70385	23,551	no
2	0,08	65	74	42231	11,538	no
2	0,1	52	66	52789	14,422	no
2	0,2	29	47	95980	28,844	no

Table 33. Parameters for turbine from Cordier diagram with B = 5,5 mm

A2. Main parameters of the pump engine

b = 4 mm						
Ψ	**φ**	**d_{in} (mm)**	**d_{out} (mm)**	**N (1/min)**	**Cm (m/s)**	**$d_{out} > d_{in}$?**
1,5	0,1	15	14	27072	2,098	no
1,5	0,08	17	17	24214	1,678	no
1,5	0,06	19	23	20970	1,259	yes
1,5	0,05	21	27	19143	1,049	yes
1,5	0,04	23	34	17122	0,839	yes
1,5	0,03	27	46	14828	0,629	yes
1,5	0,02	33	68	12107	0,42	yes
1	0,08	15	14	32820	2,055	no
1	0,06	17	19	28423	1,541	yes
1	0,05	19	22	25947	1,285	yes
1	0,04	21	28	23207	1,028	yes
1	0,03	24	37	20098	0,771	yes
1	0,02	30	56	16410	0,514	yes
0,8	0,06	16	17	33601	1,723	yes
0,8	0,05	18	20	30673	1,436	yes
0,8	0,04	20	25	27435	1,149	yes
0,8	0,03	23	33	23760	0,862	yes
0,8	0,02	28	30	19400	0,574	yes
0,8	0,01	40	100	13718	0,287	yes

Table 34. Parameters for the pump from Cordier diagram with b = 4 mm.

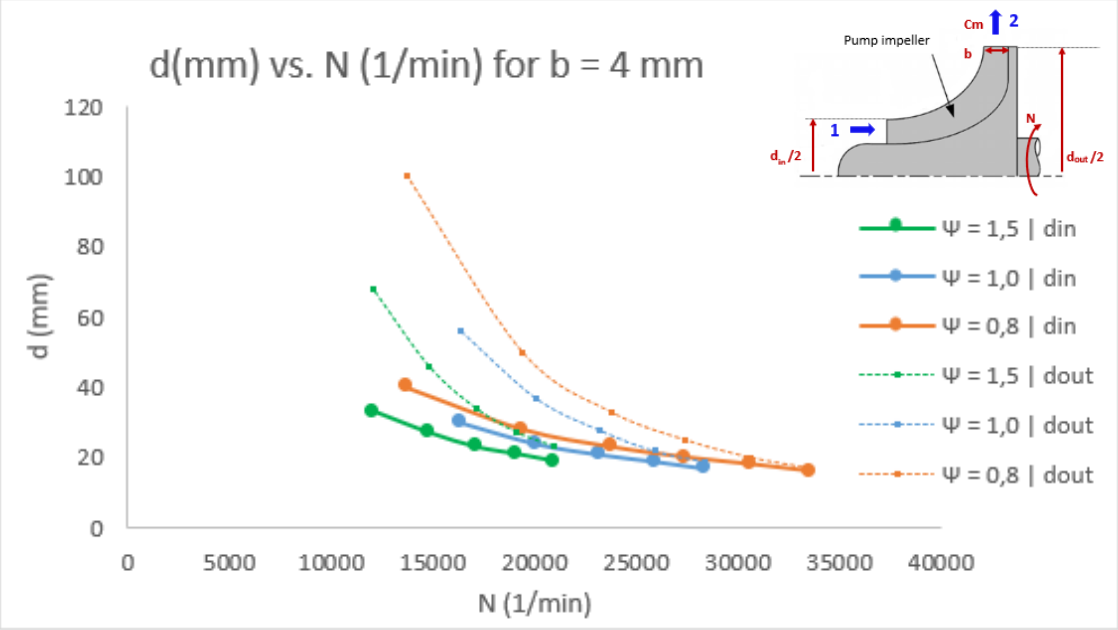

Figure 44. Combination of d(mm) and N(1/min) posible for b = 4 mm in the pump.

b = 4,5 mm						
Ψ	**φ**	**d_{in} (mm)**	**d_{out} (mm)**	**N (1/min)**	**Cm (m/s)**	**$d_{out} > d_{in}$?**
1,5	0,1	15	12	27072	2,098	no
1,5	0,08	17	15	24214	1,678	no
1,5	0,06	19	20	20970	1,259	yes
1,5	0,05	21	24	19143	1,049	yes
1,5	0,04	23	30	17122	0,839	yes
1,5	0,03	27	41	14828	0,629	yes
1,5	0,02	33	61	12107	0,42	yes
1	0,08	15	12	32820	2,055	no
1	0,06	17	17	28423	1,541	no
1	0,05	19	20	25947	1,285	yes
1	0,04	21	25	23207	1,028	yes
1	0,03	24	33	20098	0,771	yes
1	0,02	30	50	16410	0,514	yes
0,8	0,06	16	15	33601	1,723	no
0,8	0,05	18	18	30673	1,436	no
0,8	0,04	20	22	27435	1,149	yes
0,8	0,03	23	30	23760	0,862	yes
0,8	0,02	28	44	19400	0,574	yes
0,8	0,01	40	89	13718	0,287	yes

Table 35. Parameters for the pump from Cordier diagram with b = 4,5 mm.

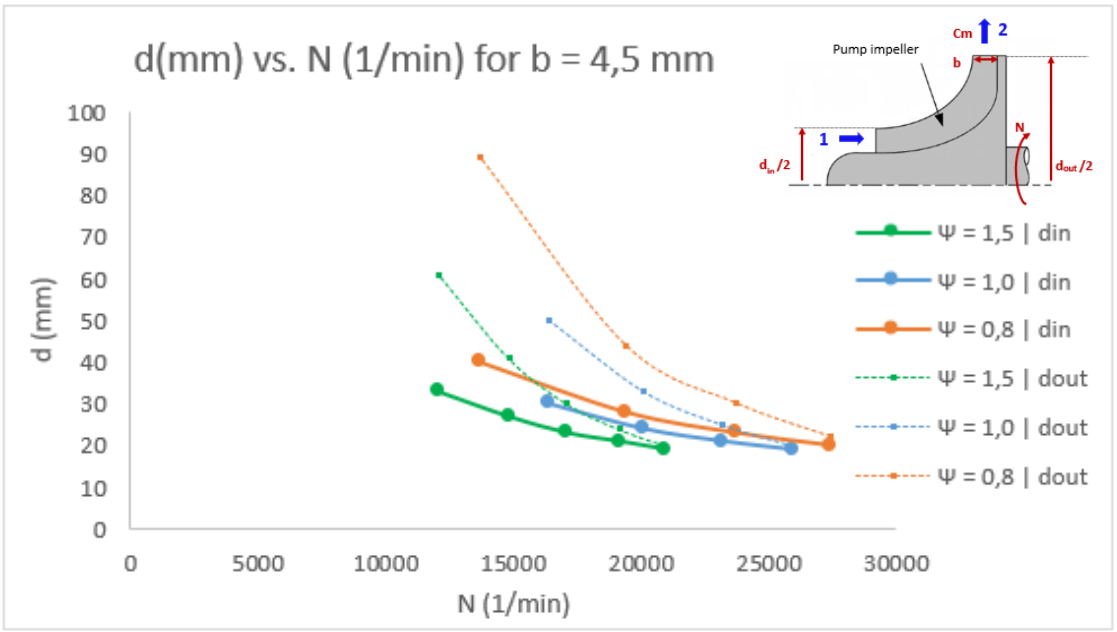

Figure 45. Combination of d(mm) and N(1/min) possible for b = 4,5 mm in the pump.

b = 5 mm						
Ψ	**φ**	**d_{in} (mm)**	**d_{out} (mm)**	**N (1/min)**	**Cm (m/s)**	**$d_{out} > d_{in}$?**
1,5	0,1	15	11	27072	2,098	no
1,5	0,08	17	14	24214	1,678	no
1,5	0,06	19	18	20970	1,259	no
1,5	0,05	21	22	19143	1,049	yes
1,5	0,04	23	27	17122	0,839	yes
1,5	0,03	27	36	14828	0,629	yes
1,5	0,02	33	55	12107	0,42	yes
1	0,08	15	11	32820	2,055	no
1	0,06	17	15	28423	1,541	no
1	0,05	19	18	25947	1,285	no
1	0,04	21	22	23207	1,028	yes
1	0,03	24	30	20098	0,771	yes
1	0,02	30	43	16410	0,514	yes
0,8	0,06	16	13	33601	1,723	no
0,8	0,05	18	16	30673	1,436	no
0,8	0,04	20	20	27435	1,149	no
0,8	0,03	23	27	23760	0,862	yes
0,8	0,02	28	40	19400	0,574	yes
0,8	0,01	40	80	13718	0,287	yes

Table 36. Parameters for the pump from Cordier diagram with b = 5 mm.

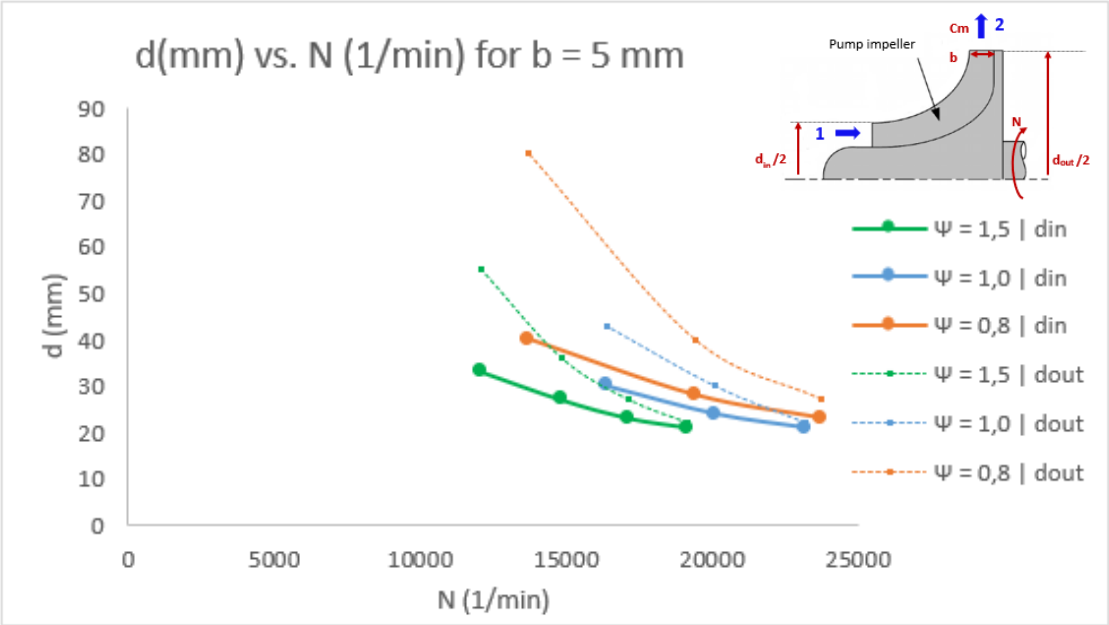

Figure 46. Combination of d(mm) and N(1/min) possible for b = 5 mm in the pump.

b = 5,5 mm						
Ψ	**φ**	**d_{in} (mm)**	**d_{out} (mm)**	**N (1/min)**	**Cm (m/s)**	**$d_{out} > d_{in}$?**
1,5	0,1	15	10	27072	2,098	no
1,5	0,08	17	12	24214	1,678	no
1,5	0,06	19	17	20970	1,259	no
1,5	0,05	21	20	19143	1,049	no
1,5	0,04	23	25	17122	0,839	yes
1,5	0,03	27	33	14828	0,629	yes
1,5	0,02	33	50	12107	0,42	yes
1	0,08	15	10	32820	2,055	no
1	0,06	17	14	28423	1,541	no
1	0,05	19	16	25947	1,285	no
1	0,04	21	20	23207	1,028	no
1	0,03	24	27	20098	0,771	yes
1	0,02	30	41	16410	0,514	yes
0,8	0,06	16	12	33601	1,723	no
0,8	0,05	18	15	30673	1,436	no
0,8	0,04	20	18	27435	1,149	no
0,8	0,03	23	24	23760	0,862	yes
0,8	0,02	28	36	19400	0,574	yes
0,8	0,01	40	73	13718	0,287	yes

Table 37. Parameters for the pump from Cordier diagram with b = 5,5 mm.

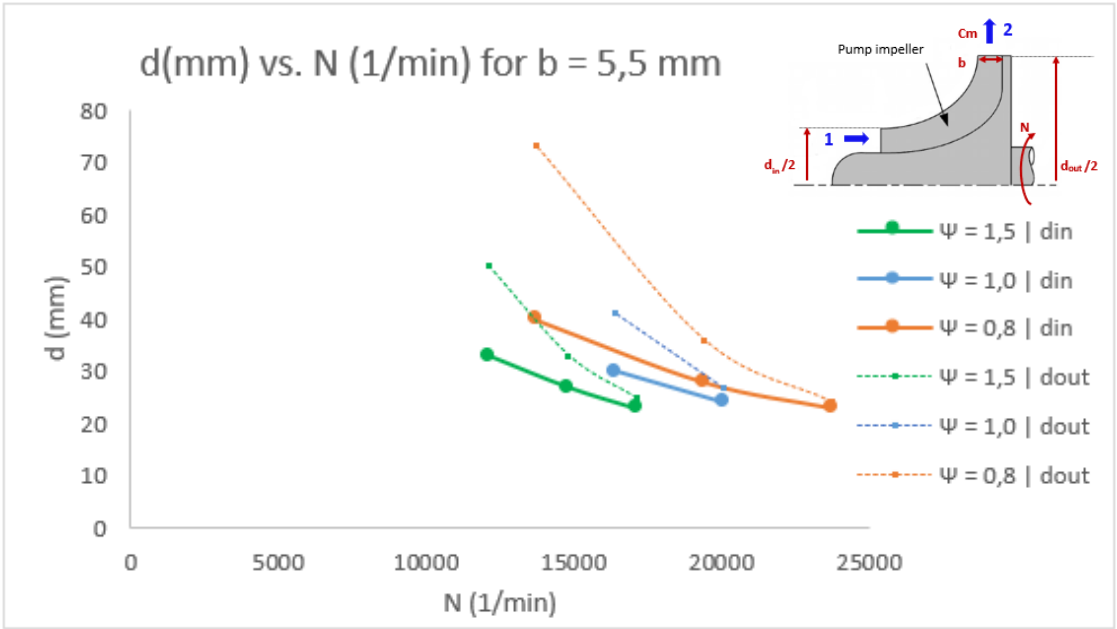

Figure 47. Combination of d(mm) and N(1/min) for b = 5,5mm in the pump.